



# Modelling potential yield capacity in conifers using Swedish long-term experiments

Alex Appiah Mensah<sup>a,\*</sup>, Emma Holmström<sup>b</sup>, Kenneth Nyström<sup>a</sup>, Urban Nilsson<sup>b</sup>

<sup>a</sup> Department of Forest Resource Management, Swedish University of Agricultural Sciences, SE-901 83 Umeå, Sweden

<sup>b</sup> Southern Swedish Forest Research Centre, Swedish University of Agricultural Sciences, SE-230 53 Alnarp, Sweden

## ARTICLE INFO

### Keywords:

Forest site productivity  
Site index  
Yield capacity  
Regression  
Boreal forest  
Climate change

## ABSTRACT

Information on forest site productivity is a key component to assess the carbon sequestration potential of boreal forests. While site index (SI) is commonly used to indicate forest site productivity, expressions of SI in the form of yield capacity (potential maximum mean annual volume increment) is desirable since volume yield is central to the economic and ecological analyses of a given species and site. This paper assessed the functional relationship between SI and yield capacity on the basis of yield plot data from long-term experiments measured over several decades for Norway spruce (*Picea abies*), Scots pine (*Pinus sylvestris*), Lodgepole pine (*Pinus contorta*) and Larch (*Larix decidua* and *Larix sibirica*) in Sweden. Component models of total basal area and volume yield were also developed. SI was determined by existing height development functions using top height and age, whereas functions for stand-level ( $\text{m}^2 \text{ha}^{-1}$ ) basal area development were constructed based on age, SI and initial stand density using difference equations and nonlinear mixed-effects models. The relation between volume yield ( $\text{m}^3 \text{ha}^{-1}$ ) and top height was adjusted with total basal area production through nonlinear mixed-effects models. Species-specific parametric regression models were used to construct functional relationships between SI and yield capacity. The root mean square errors of the species-specific models ranged from 2 to 6% and 10–18% of the average values for the basal area and volume equations, respectively. For the yield capacity functions, the explained variations ( $R^2$ ) were within 80–96%. We compared our yield capacity functions to earlier functions of the species and significant differences were observed in both lower and higher SI classes, especially, for Scots pine and Norway spruce. The new functions give better prediction of yield capacity in current growing conditions; hence, they could later be used for comparing tree species' production under similar site and management regimes in Sweden.

## 1. Introduction

The rate of forest growth is an important component of the boreal forest carbon stocks' balance. Recent reports have shown forest management- and environment- induced growth increase, for example, in the boreal forests of northern Europe (e.g. Sharma et al., 2012; Kauppi et al., 2014; Henttonen et al., 2017; Appiah Mensah et al., 2021; Mäkinen et al., 2021). Thus, the boreal forest is a critical component of the global carbon cycle and its health (growth and productivity) is of primary concern (Gauthier et al., 2015). Valid data and new expressions for forest site productivity in growth models are needed for unbiased assessments of management and environmental impacts on the growth and carbon fluxes of boreal forests in the short- and long-term horizons

(Boisvenue and Running, 2006; Skovsgaard and Vanclay, 2008; Fontes et al., 2010; Bontemps and Bouriaud, 2014).

Information on site productivity is also needed by foresters in many ways, for example, to plan silvicultural treatments across the rotation period, to forecast forest growth and to quantify wood biomass production potential from local-to-regional and- national scales (Pretzsch et al., 2008). Site productivity may also be important when to assess biodiversity and other ecosystem services in relation to forest management (e.g. Felton et al., 2017, 2019). In Sweden, the site productivity is also the legislative boundary of the Forestry Act, and only forestlands where the average annual potential wood production exceeds  $1 \text{ m}^3 \text{ha}^{-1} \text{yr}^{-1}$  are considered as productive forest land. On poorer sites, no harvest is allowed and Swedish national statistics are reported differently based

\* Corresponding author.

E-mail addresses: [alex.appiah.mensah@slu.se](mailto:alex.appiah.mensah@slu.se) (A.A. Mensah), [emma.holmstrom@slu.se](mailto:emma.holmstrom@slu.se) (E. Holmström), [Kenneth.Nystrom@slu.se](mailto:Kenneth.Nystrom@slu.se) (K. Nyström), [Urban.Nilsson@slu.se](mailto:Urban.Nilsson@slu.se) (U. Nilsson).

<https://doi.org/10.1016/j.foreco.2022.120162>

Received 14 January 2022; Received in revised form 7 March 2022; Accepted 9 March 2022

Available online 16 March 2022

0378-1127/© 2022 The Author(s). Published by Elsevier B.V. This is an open access article under the CC BY license (<http://creativecommons.org/licenses/by/4.0/>).

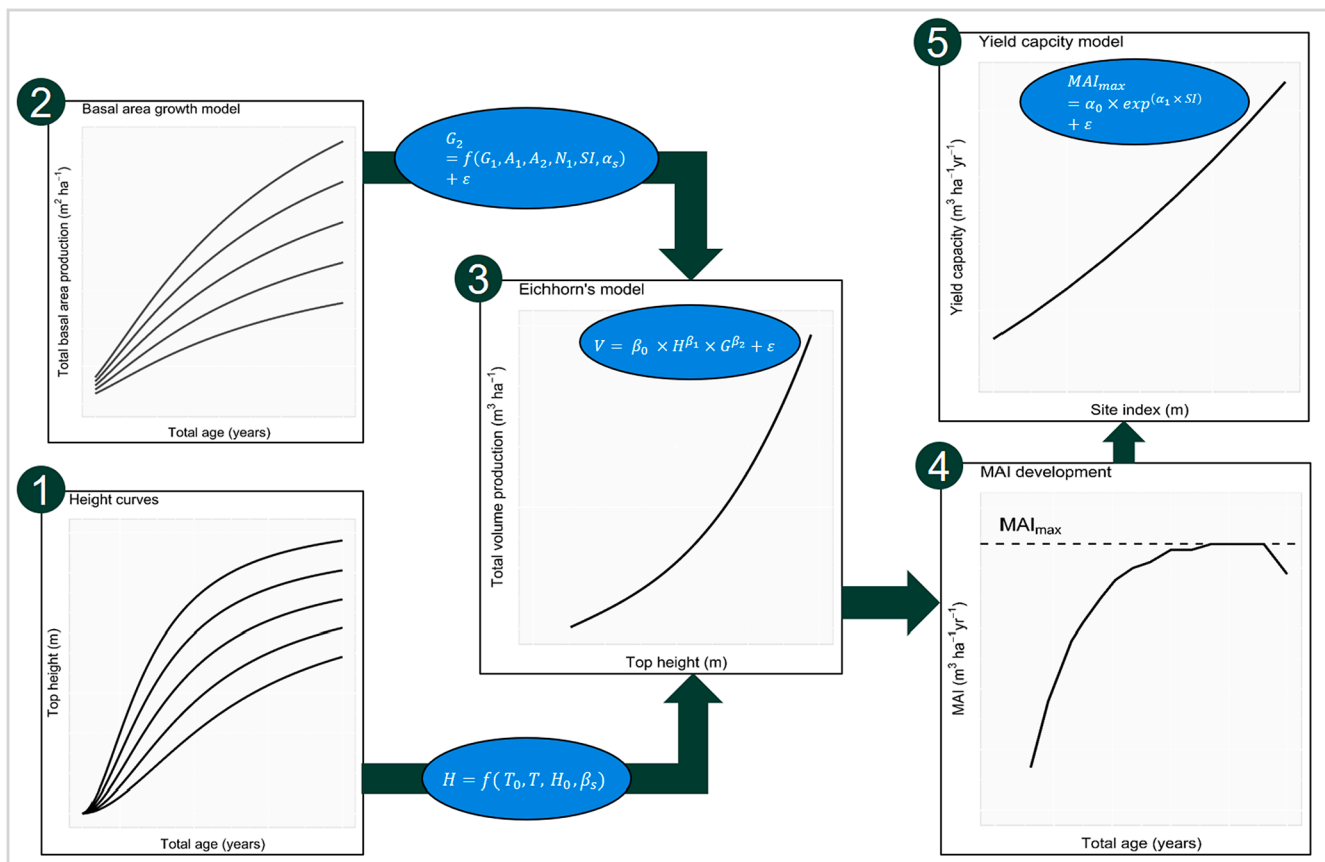


Fig. 1. Stepwise estimation of yield capacity in this study. The elongated circles denote the models applied at each step.

on this boundary (Nilsson, 2020).

Forest site productivity is generally defined as the potential of a site to produce wood biomass or tree volume (Skovsgaard and Vanclay, 2008). It is assessed by several methods that can be broadly grouped into two: geocentric and phytocentric. The geocentric methods are mostly based on site indicators of climate, topography and soil, whereas the phytocentric methods are vegetation related, made up of tree- or plant-based indicators (Hägglund, 1981; Skovsgaard and Vanclay, 2008). The two methods have been widely applied in studies on forest site productivity assessment for several tree species across biomes (e.g. Hägglund and Lundmark, 1977; Szwaluk and Strong, 2003; Mason et al., 2017; Bueis et al., 2019; Eckhart et al., 2019; Liu et al., 2021).

Site index (SI), defined as the height attained at a reference age is the most commonly used indicator of forest site productivity. In Sweden, SI is generally estimated in three ways: (1) by height development curves, (2) by site factors (combination of climate, soil, field and bottom vegetation) and (3) by intercept method. Method 1 is used for matured stands (above 20 years), while method 3 is applied mainly in young stands (below 20 years). Method 2 can be applied on all forestlands and is used by the National Forest Inventory to estimate SI (Hägglund and Lundmark, 1977; Elfving and Kiviste, 1997; Nilsson, 2020). For even-aged monoculture stands, SI based on height development curves (height-age relations) of the dominant trees is often desirable when estimating the potential of the growing site. This is because height growth is strongly related to volume production, and the height growth of the largest trees is relatively independent of stand density and thinning from below treatments (Eichhorn, 1902; Skovsgaard and Vanclay, 2008; Burkhardt and Tomé, 2012). However, expressing SI in terms of the potential average volume yield produced over the stand rotation is desired since timber volume is a key parameter in economic and ecological analyses of forest resources. Hence, for even-aged forest stands, the relation between SI and maximum mean annual volume

increment (hereafter, referred to as yield capacity) can directly be used to describe the potential amount of wood volume that can be obtained per year on a site for a given species (Hägglund, 1981; Hägglund and Lundmark, 1982; Elfving and Nyström, 1996) and for further classification of forest lands as productive and unproductive units.

Nevertheless, the relation between SI and yield capacity is not always straightforward, especially when the methods used rely on the general Eichhorn's law (Eichhorn, 1902). The law stipulates that stands have the same total volume yield when they reach the same dominant height, independent of age and SI (Eichhorn, 1902). However, under comparable management regimes, the total volume yield over the rotation has been shown to vary within the same SI for several species including Norway spruce (*Picea abies*) by Assmann (1955), Scots pine (*Pinus sylvestris*) by Schmidt (1973) and loblolly pine (*Pinus taeda*) by Hasenauer et al. (1994). Therefore, for a given species and management regime, significant site-dependent variations may occur in the yield levels (total volume production at a given height), suggesting that stands of different yield levels may have different trajectories for height-volume relations across the rotation period (Assmann, 1970; Hasenauer et al., 1994; Skovsgaard, 1997). Including variables that capture the variations in yield levels can therefore improve estimates of yield capacity and enhance meaningful comparisons across species, sites and regions (Skovsgaard and Vanclay, 2008; Ekö et al., 2008). Differences in yield levels are attributable to many factors such as climate, soil, seed provenance, silviculture, stand density, basal area production and form factors (Skovsgaard and Vanclay, 2008). Basal area production as a measure of potential density has been found to explain larger variations in the volume yield levels and thus, provide satisfactory outcomes of site productivity assessment (Assmann, 1966; Sterba, 1987; Ung and Ouellet, 1991; Hasenauer et al., 1994; Sterba and Monserud, 1995; Hall et al., 2019; Allen et al., 2020).

The maturation of long-term yield experiments (LTEs) of tree species

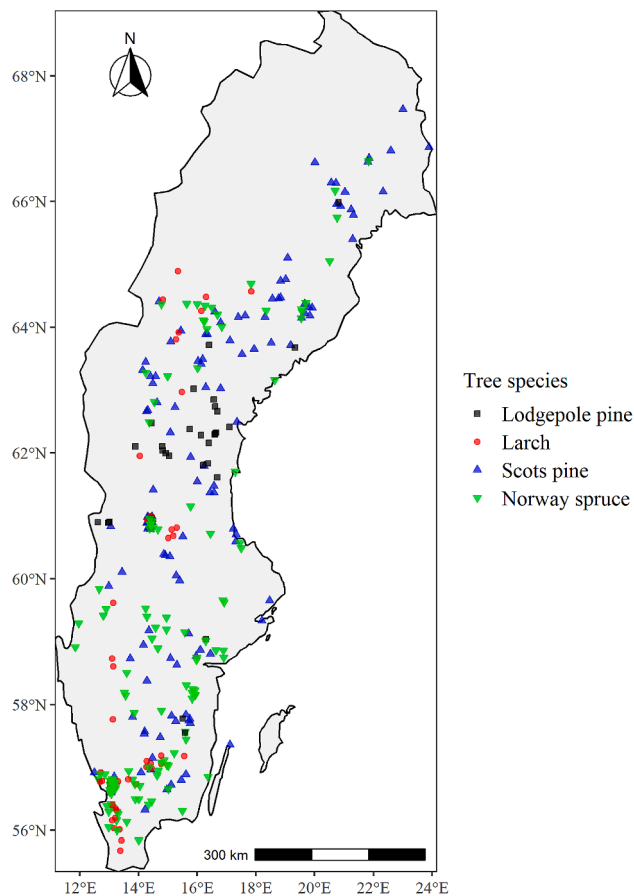


Fig. 2. Locations of LTE sites for the different tree species in Sweden.

where height development, carrying capacity (described by total basal area production) and total stem volume produced over time could be easily and reliably estimated provides a unique insight into the evaluation of yield capacity by using SI (Pretzsch et al., 2019). In Sweden, LTEs were established throughout the country in the 20th century to provide quantitative results for forest management planning (e.g. Elfving, 2010a; Nilsson et al., 2010). Now, tree growth data in the LTEs have

accumulated and this paper presents an investigation of site productivity for the major tree species under Swedish conditions.

The general objective of the study was to improve the estimates of yield capacities for major forest tree species in Sweden. The specific objectives were two fold; (i) to develop functional relationships between yield capacity and SI predicted by height curves using data from LTEs, and (ii) to compare the estimated yield capacities with those predicted by earlier functions from Hägglund and Lundmark (1982) for forest tree species in Sweden.

The study was limited to the tree species where we had measured data series from unthinned and thinned (from below) stands and with measurements of total volume production including mortality, harvest removals and standing volume, which resulted in four species being selected: Norway spruce (*Picea abies*), Scots pine (*Pinus sylvestris*), Lodgepole pine (*Pinus contorta*) and Larch (*Larix decidua* – European Larch and *Larix sibirica* – Siberian Larch). Together, these species contribute more than 80% to the total growing stock volume on forest lands in Sweden (Nilsson, 2020).

## 2. Material and methods

The study approach was generally centred on the principles of forest yield production (Fig. 1). The stepwise approach was carried out in five main steps: based on height development (1) and corresponding basal area development (2), total volume production was estimated (3). Yield capacity was then derived from volume yield and age (4), and functional relationships between yield capacity and site index were established (5). The constructed yield capacity functions in the present study were compared to earlier functions and the observed differences were discussed in relation to methodological approaches and changes in environmental conditions. The five modelling steps are expanded in the following sub-sections.

### 2.1. Data

The data material comprised LTEs from 330 locations in Sweden (Scots pine = 169, Norway spruce = 86, Lodgepole pine = 34, Larch = 41). All selected LTEs were originally experiments in block designs where the total production (yield) was recorded, including mortality, harvest removals and standing volume. The sites covered a wide range of fertility, latitudinal and altitudinal gradients in Sweden (Fig. 2; Table 1). For each site, only the control and thinned-from-below plots with

Table 1  
Summary of stand and site data for included plots.

| Tree species   |      | Age (years) | Top height (m) | Basal area (m <sup>2</sup> ha <sup>-1</sup> ) | Volume (m <sup>3</sup> ha <sup>-1</sup> ) | Stand density (trees ha <sup>-1</sup> ) | Site index (m) | Thinning ratio | Measurement year | Latitude (°N) | Altitude (m a.s.l) | No. LTEs (plots) | N    |
|----------------|------|-------------|----------------|---|---|---|----------------|----------------|------------------|---------------|--------------------|------------------|------|
| Scots pine     | min  | 10          | 2              | 0.7   | 0.7                                       | 300                                     | 13             | 0              | First: 1927      | 56            | 0                  |                  |      |
|                | mean | 46          | 14             | 29  | 207                                       | 2116                                    | 24             | 0.09           | –                | –             | 207                | 169              | 4498 |
|                | max  | 119         | 31             | 105   | 1169                                      | 15,867                                  | 32             | 0.95           | Latest: 2018     | 67            | 560                | (981)            |      |
| Norway spruce  | min  | 12          | 2              | 0.8   | 0.2                                       | 433                                     | 16             | 0              | First: 1928      | 55            | 3                  |                  |      |
|                | mean | 42          | 16             | 35  | 327                                       | 2615                                    | 29             | 0.04           | –                | –             | 136                | 86               | 2022 |
|                | max  | 133         | 37             | 140   | 1608                                      | 13,106                                  | 36             | 0.95           | Latest: 2018     | 66            | 610                | (427)            |      |
| Lodgepole pine | min  | 15          | 4              | 4   | 2   | 333                                     | 16             | 0              | First: 1953      | 56            | 0                  |                  |      |
|                | mean | 33          | 14             | 29  | 211                                       | 2028                                    | 22             | 0.03           | –                | –             | 291                | 34               | 742  |
|                | max  | 83          | 26             | 72  | 700                                       | 9062                                    | 30             | 0.95           | Latest: 2019     | 69            | 480                | (273)            |      |
| Larch spp.     | min  | 6           | 3              | 0.1   | 0.9                                       | 355                                     | 24             | 0              | First: 1949      | 55            | 20                 |                  |      |
|                | mean | 32          | 19             | 36  | 311                                       | 1923                                    | 36             | 0.23           | –                | –             | 160                | 41               | 462  |
|                | max  | 104         | 35             | 94  | 1043                                      | 11,687                                  | 42             | 0.95           | Latest: 2019     | 64            | 435                | (108)            |      |

min: minimum; max: maximum; thinning form describes unthinned plots (0) and thinned from below plots (1)≤; N is the total number of measurements.

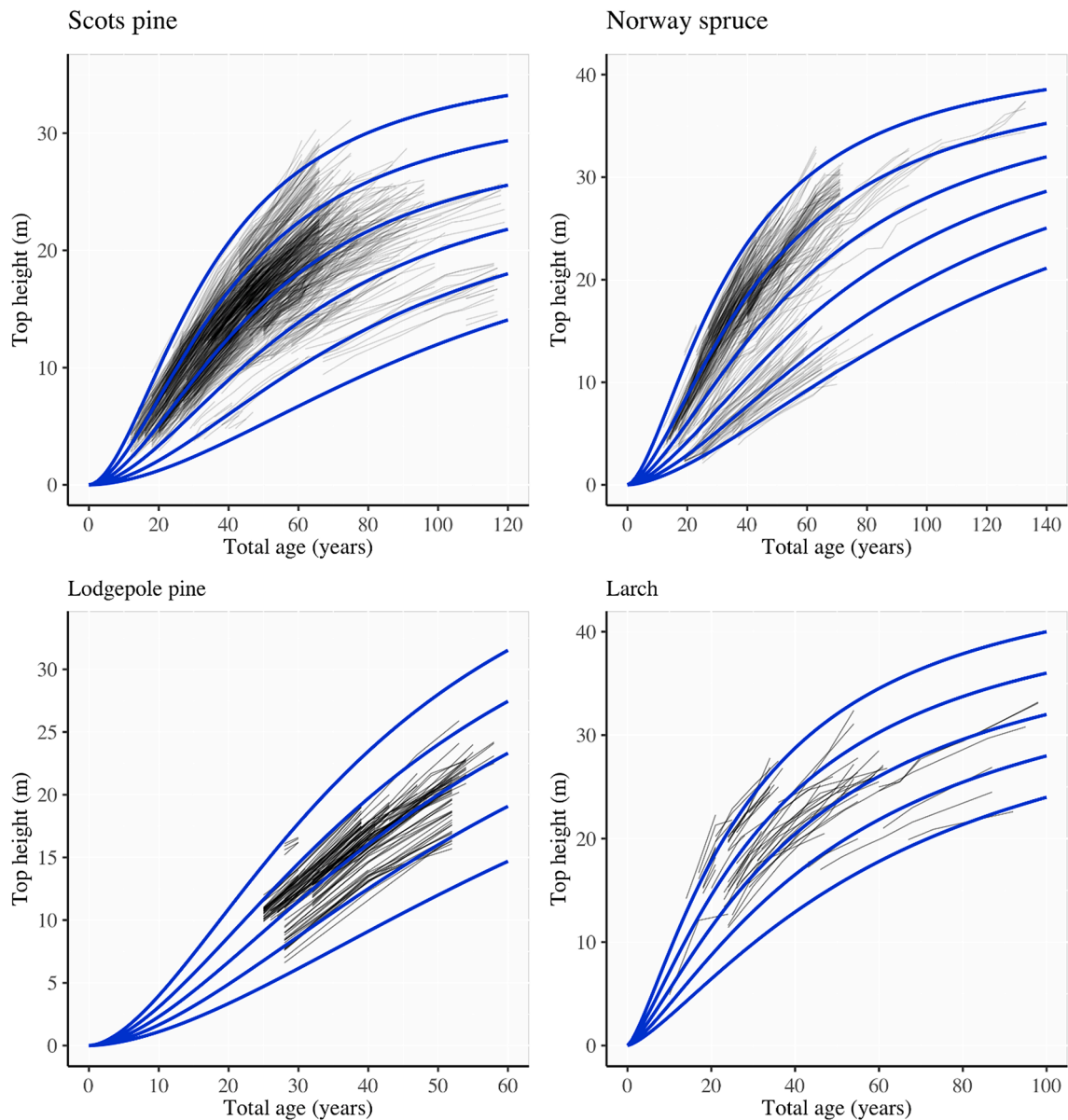


Fig. 3. Observed height development (black lines) in relation to site index curves (blue lines). (For interpretation of the references to colour in this figure legend, the reader is referred to the web version of this article.)

thinning grade (percent removed basal area) < 35% and thinning ratio < 0.95 were used for the yield analyses. Thinning ratio is expressed by the quotient between the basal area mean diameters of removed and remaining trees. Fertilised plots were excluded from the dataset. The studied plots were fully stocked even-aged stands where more than 70% of the total basal area consisted of the main tree species. For most sites, plot measurements had been conducted between 1920 and 2019, with irregular measurement intervals. The remeasurement interval was on average 8 years and the frequency of remeasurements on a plot ranged from 2 to 14 times. Permanent square or rectangular sample plots with net sizes of approximately 0.1 ha were used to collect the tree information. Total age, tree species and damages were recorded in addition to perpendicularly calipered tree diameters at breast height (1.3 m from the ground). Trees were numbered at first measurement to ensure that remeasurements in subsequent years could be linked to the same individual trees.

Among the trees recorded on the plot, a sub-sample was taken for total height measurement using the Tiréns device before 1970, Suunto hypsometer 1970–1995 and the Haglöf Vertex hypsometer afterwards.

Sample trees were followed over time for total height, except for cases of damages by storm, snow, diseases, etc., in which they were replaced by equally good candidates. The observations of height-diameter pairs were used to estimate coefficients of the height-diameter equation (Eq. (1)) presented by Näslund (1947), where coefficients were estimated for each plot and measurement occasion, and all calipered trees without heights were assigned predicted heights. Based on the predicted heights, the thickest trees on every plot were selected as the top (dominant) height trees. Top height was defined as the arithmetic mean height of the 100 thickest (by diameter) trees  $\text{ha}^{-1}$ . The initial stand densities (trees  $\text{ha}^{-1}$ ) during installation of the plots as well as site information were recorded. Other variables such as basal area and stem volume were computed for every calipered tree and aggregated to the plot level in per hectare units. The tree volume was estimated for living, thinned and dead trees using the species-specific volume functions by Brandel (1990). Summary of the plot and site variables are given in Table 1.

$$H = \frac{DBH^\alpha}{(\alpha + \beta \times DBH)^\gamma} + 1.3 \quad (1)$$

**Table 2**  
Tested total basal area development functions.

| No. | Equation   |
|-----|--|
| F01 | $G_{ijk} = \exp \left[ \ln(G_{ijl}) + \mu + \alpha_0 \left( \frac{1}{A_{ijk}} - \frac{1}{A_{ijl}} \right) + \mu + \alpha_1 (N_1) + \mu + \alpha_2 (SI) \right] + \varepsilon_{ijk}$  |
| F02 | $G_{ijk} = \frac{1}{\left[ \left( \frac{1}{G_{ijl}} \right) \left( \frac{A_{ijl}}{A_{ijk}} \right)^{\alpha_0 + \mu} + \mu + c_0 \left( 1 - \left( \frac{A_{ijl}}{A_{ijk}} \right)^{\alpha_0 + \mu} \right) + \mu + \alpha_1 (N_1) + \mu + \alpha_2 (SI) \right]} + \varepsilon_{ijk}$              |
| F03 | $G_{ijk} = \left[ \left( G_{ijl} \right)^{\mu + c_0} \left( \frac{A_{ijl}}{A_{ijk}} \right)^2 + \mu + \alpha_0 \left( 1 - \left( \frac{A_{ijl}}{A_{ijk}} \right)^2 \right) \right]^{\frac{1}{c_0 + \mu} + \mu + \alpha_1 (N_1) + \mu + \alpha_2 (SI)} + \varepsilon_{ijk}$                         |
| F04 | $G_{ijk} = \left[ G_{ijl} \left( \frac{1 - \exp^{\mu - \alpha_0 (A_{ijk})}}{1 - \exp^{\mu - \alpha_0 (A_{ijl})}} \right)^{\mu + c_0 + \mu + \alpha_1 (N_1) + \mu + \alpha_2 (SI)} \right] + \varepsilon_{ijk}$   |
| F05 | $G_{ijk} = \left[ \exp \left( \ln(G_{ijl}) \left( \frac{A_{ijl}}{A_{ijk}} \right)^{\mu + \alpha_0 + \mu + \alpha_1 (N_1)} + \mu + \alpha_2 (SI) + \mu + c_0 \left( 1 - \left( \frac{A_{ijl}}{A_{ijk}} \right)^{\mu + \alpha_0 + \mu + \alpha_1 (N_1)} \right) \right) \right] + \varepsilon_{ijk}$ |

**Table 3**  
Summary of fit-statistics for the tested basal area functions. Relative RMSEs and MDs are given in parenthesis. The selected model for each species is highlighted in bold.

|     |          | Scots pine    | Norway spruce | Lodgepole pine | Larch          |
|-----|----------|---------------|---------------|----------------|----------------|
| F01 | RMSE (%) | 1.09 (3.39)   | 0.97 (2.14)   | 1.31 (3.35)    | 3.40 (7.04)    |
|     | MD (%)   | -0.15 (-0.47) | -0.10 (-0.22) | -0.12 (-0.33)  | -0.65 (1.36)   |
| F02 | RMSE (%) | 2.68 (8.32)   | 2.73 (6.04)   | 1.57 (4.23)    | 6.37 (13.2)    |
|     | MD (%)   | -0.06 (-0.19) | -1.33 (-2.95) | -0.60 (1.61)   | -5.25 (10.87)  |
| F03 | RMSE (%) | 3.42 (10.63)  | 1.90 (4.21)   | 3.10 (8.34)    | 10.56 (18.31)  |
|     | MD (%)   | 1.66 (5.15)   | 0.14 (0.31)   | 2.37 (6.38)    | -8.33 (-24.75) |
| F04 | RMSE (%) | 2.53 (7.86)   | 1.82 (4.03)   | 1.22 (3.29)    | 2.79 (5.78)    |
|     | MD (%)   | 0.26 (0.82)   | -0.09 (-0.20) | -0.01 (-0.03)  | -0.29 (-0.59)  |
| F05 | RMSE (%) | 3.29 (10.22)  | 1.96 (4.32)   | 1.94 (5.21)    | 3.68 (7.58)    |
|     | MD (%)   | 0.04 (0.12)   | -0.11 (-0.55) | 1.00 (2.69)    | 0.05 (0.11)    |

where,  $H$  is the tree height (m),  $DBH$  is the calipered tree diameter at breast height (cm),  $\alpha$ ,  $\beta$  are parameters to be estimated and  $\gamma$  was 3 for Norway spruce and 2 for other tree species (to minimize the sum of squared residuals).

### 2.2. Site index estimation from height development curves

The SI functions operationally used today in Sweden were used to estimate SI from the observed top heights on each plot and thereafter, averaged to provide the SI for each site (experiment location). More information concerning the form and parameter estimates of the SI functions can be found in [Elfving and Kiviste \(1997\)](#), [Elfving \(2009\)](#) and [Liziniwicz et al. \(2016\)](#). SI was defined as the mean top height at the tree species-specific reference age (100 years:  $H_{100}$ , for Norway spruce, Scots pine and Larch; and 50 years:  $H_{50}$ , for Lodgepole pine). Preliminary assessment showed that the SI curves adequately described the patterns in the observed top height development for all species ([Fig. 3](#)). With a given plot SI, we derived the expected mean top heights at ages corresponding to the observed measurement years, assuming the growth function passes through current height and age. The expected top

heights were used to simulate the expected plot-level total volume productions (see [Fig. 1](#) and Section 2.4).

### 2.3. Functions for total basal area development

Basal area is often used to describe stands' potential density (carrying capacity) and due to its strong relationship with stem volume and woody biomass production, it is of central significance to modelling forest stand development ([Burkhardt and Tomé, 2012](#)). To determine the carrying capacity of forest stands, projections of basal area growth require repeated observations from plots covering gradients in stand and environmental conditions ([Gadow and Hui, 1999](#)).

Studies from long-term spacing trials shown the significant influence of initial spacing on stand productivity ([Pettersson, 1992](#); [Samuelsson et al., 2010](#)), and as such the basal area growth increases asymptotically with age and the asymptote is largely dependent on site quality and initial stand density ([Pienaar and Shiver, 1986](#); [Elfving, 2010a](#); [Hall et al., 2019](#)). Hence, the following growth functions ([Table 2](#)) were used to examine the development of total basal area production (including surviving, removed and dead trees) for the different tree species. Model one (F01) is identical to [Pienaar et al. \(1990\)](#), F02 is based on Hossfeld ([Peschel, 1938](#)), F03 is based on Levakovic ([Levakovic, 1935](#)), F04 is based on Bertalanffy-Richards ([von Bertalanffy, 1938](#); [Richards, 1959](#)) and F05 is derived from Schumacher's growth function ([Schumacher, 1939](#)).

Under a model-based framework, the yield function relates the response variable (total basal area,  $m^2 ha^{-1}$ ) to a set of independent variables and was expressed generally as

$$y_i = f(X_i; B) + \varepsilon_i \tag{2.1}$$

where  $i$  indexes the population units;  $y_i$  is the observation of the response variable on the  $i$ th unit;  $X_i$  is a vector of predictor variables comprising total age (years), site index (m) and initial stand density (trees  $ha^{-1}$ );  $B$  is a vector of parameters to be estimated from the sample data;  $f(X_i; B)$  expresses the nonlinear relationship between predictor variables and the parameters; and  $\varepsilon_i$  is a normally distributed random residual term [ $\varepsilon_i \sim N(0, \sigma^2)$ ] to account for the unexplained variation in the observed values of  $y_i$ . Given repeated plot measurements, difference equations are more suitable for modelling the dynamics of yield within an observed growth period and as such, produce robust base-age invariant results compared to static base-age equations ([Cieszewski and Bailey, 2000](#)). Therefore, Eq. (2.1) was expressed in an algebraic difference form (Eq. (2.2)) where the basal area at time two ( $G_2$ ) was modelled from the basal area at time one ( $G_1$ ), total age at times one ( $A_1$ ) and two ( $A_2$ ), site index ( $SI$ ) and initial stand density ( $N_1$ ).

$$G_2 = f(G_1, A_1, A_2, N_1, SI, \alpha_s) + \varepsilon_i \tag{2.2}$$

where  $N_1$  was transformed as:  $N_1 = \sqrt{\frac{10000}{N}}$  and the  $\alpha_s$  are model parameters.

The tested functions (F01-F05) have polymorphic asymptotes and their difference forms are presented in [Table 2](#). We used all measurements within the observed growth period to model the basal area growth. The growth period was defined as the time interval between consecutive measurements. The sample data for model fitting were hierarchical in structure, i.e., several plots nested within a site. The plots had many revisions, which suggest observations within a plot might exhibit temporal dependencies. Similarly, the distance between sample plots within each site is small (about 20–500 m apart) and this may induce a spatial autocorrelation among observations from a site. The lack of independency among observations may violate standard regression analysis through biased model parameter estimates and subsequently, lead to erroneous inferences. Hence, the tested basal area growth equations were expressed as nonlinear mixed-effects time series models to account for both plot and site random variances ([Gregoire and](#)

**Table 4**

Parameter estimates of species-specific basal area ( $m^2 ha^{-1}$ ) functions. Values in parenthesis are estimated standard errors.

| Class                                    | Parameter                                       | Scots pine             | Norway spruce          | Lodgepole pine   | Larch                  |
|--|---|------------------------|------------------------|------------------|------------------------|
|  |   | Estimates              |                        |                  |                        |
| Fixed effects                            | $\hat{\alpha}_0$                                | -52.8873 (1.5744)      | -55.1743 (4.2183)      | 0.0507 (0.0027)  | 0.0287 (0.0151)        |
|  | $\hat{\alpha}_1$                                | 0.0064 (0.0023)        | 0.0273 (0.0066)        | 1.0931 (0.2019)  | 0.7837 (0.2485)        |
|  | $\hat{\alpha}_2$                                | -0.0007 (0.0003)       | -0.0012 (0.0006)       | -0.1089 (0.0281) | 0.5909 (0.4267)        |
|  | $\hat{c}_0$                                     |                        |                        | 2.6904 (0.1896)  | 0.0887 (0.0302)        |
| Plot-level random effects<br>( $\mu_p$ ) | $\widehat{var}(\hat{\alpha}_0)$                 | 61.856                 | 22.242                 |                  | $1.37 \times 10^{-18}$ |
|  | $\widehat{var}(\hat{\alpha}_1)$                 | $5.89 \times 10^{-6}$  | $4.39 \times 10^{-5}$  |                  |                        |
|  | $\widehat{var}(\hat{\alpha}_2)$                 | $1.84 \times 10^{-19}$ | $4.11 \times 10^{-7}$  | 0.0028           |                        |
|  | $\widehat{cov}(\hat{\alpha}_0, \hat{\alpha}_1)$ | 0.0164                 | -0.0291                |                  |                        |
|  | $\widehat{cov}(\hat{\alpha}_0, \hat{\alpha}_2)$ | 0                      | 0.0029                 |                  |                        |
|  | $\widehat{cov}(\hat{\alpha}_1, \hat{\alpha}_2)$ | 0                      | $-4.23 \times 10^{-6}$ |                  |                        |
| Site-level random effects<br>( $\mu_s$ ) | $\widehat{var}(\hat{\alpha}_0)$                 | 285.958                | 1068.321               |                  | $3.77 \times 10^{-5}$  |
|  | $\widehat{var}(\hat{\alpha}_1)$                 | $9.817 \times 10^{-6}$ | 0.0013                 |                  |                        |
|  | $\widehat{var}(\hat{\alpha}_2)$                 | $6.371 \times 10^{-6}$ | $1.31 \times 10^{-5}$  | 0.1254           |                        |
|  | $\widehat{cov}(\hat{\alpha}_0, \hat{\alpha}_1)$ | 0.0269                 | 0.2797                 |                  |                        |
|  | $\widehat{cov}(\hat{\alpha}_0, \hat{\alpha}_2)$ | 0.0281                 | 0.0936                 |                  |                        |
|  | $\widehat{cov}(\hat{\alpha}_1, \hat{\alpha}_2)$ | $7.77 \times 10^{-6}$  | $5.33 \times 10^{-6}$  |                  |                        |
| Residual Variance<br>$V(\epsilon_{ijk})$ | $\hat{\omega}^2$                                | 4.6439                 | 2.7276                 | 837.5821         | $5.75 \times 10^5$     |
|  | $\hat{\delta}_1$                                | -0.1747                | -0.0979                | -1.4996          | -1.5454                |
|  | $\hat{\delta}_0$                                |                        |                        | 0.0382           | $1.14 \times 10^{-10}$ |
| Autocorrelation<br>$n$                   | $\hat{\rho}$                                    | 0.042                  | 0.215                  | 0.146            | 0.294                  |
|  |   | 3447                   | 984                    | 237              | 78                     |

Schabenberger, 1996; Mehtätalo and Lappi, 2020).

In Table 2,  $G_{ijk}$  is the plot basal area (at the end of the growth period) at age  $A_{ijk}$  ( $k$  th observations at plot/series  $j$  and site  $i$ ),  $G_{ijl}$  is the plot basal area (at the beginning of the growth period) at age  $A_{ijl}$  at the same plot/series and site ( $l$  th observations at plot/series  $j$  and site  $i$  and  $l \neq k$ ), the  $\mu$  denotes between group variances of the two level groups denoted as plot-level ( $\mu_p$ ) and site-level ( $\mu_s$ ) random effects, which are independent and normally distributed [ $\mu_p \sim N(0, D^*)$  and  $\mu_s \sim N(0, D^*)$ ] with between group variance-covariance matrix ( $D^*$ ) identical for all plots and sites.  $G_{ijl}$  was considered as a fixed-effect parameter and was locally estimated for each plot and site. The within group variance specified by the individual random model errors ( $\epsilon_{ijk}$ ) is normally distributed [ $\epsilon_{ijk} \sim N(0, \sigma^2)$ ] and independent among observations and  $\mu_p$  and  $\mu_s$ . The random-effects parameters were added sequentially to the fixed-effects parameters until convergence was achieved. The model parameters were estimated by approximations of the likelihood function of the Lindstrom-Bates algorithm implemented in the “nlme” package of R statistical environment (Pinheiro et al., 2020; R Core Team, 2020).

Due to unequal variances (heteroscedasticity) arising from measurements at differing stand ages and sites, the within-group random error variance [ $V(\epsilon_{ijk})$ ] associated with every predicted plot-level basal area ( $\hat{G}_{ijk}$ ) were modelled by nonlinear power models (Eqs. (3.1) and (3.2)) with either two parameters (scale and shape, denoted as  $\omega^2$  and  $\delta_1$  respectively) or three parameters ( $\omega^2$  and  $\delta_1$  plus a constant,  $\delta_0$ ). Negative ( $\delta_1 < 0$ ), or positive ( $\delta_1 > 0$ ) values of  $\delta_1$ , suggests the error variance may be decreasing or increasing linearly with  $\hat{G}_{ijk}$  (Mehtätalo and Lappi, 2020). Given that our basal area measurements were unevenly spaced over time and only one single pair of basal area-age measurement were used for basal area projection, the first order autoregressive [AR (1)] error structure (Eq. (3.3)) was chosen to account for the within-plot serial correlation.

$$V(\epsilon_{ijk}) = \omega^2 |\hat{G}_{ijk}|^{2\delta_1} \tag{3.1}$$

$$V(\epsilon_{ijk}) = \omega^2 (\delta_0 + |\hat{G}_{ijk}|^{\delta_1})^2 \tag{3.2}$$

$$\rho^z = cor(\epsilon_{ijk} + \epsilon_{ijk+z}) \tag{3.3}$$

where  $\rho$  the correlation between successive observations is a parameter to be estimated and  $z$  is a time lag in terms of measurement intervals between successive observations in the same plot. The accuracy of the tested basal area models were compared using the following estimators (Eqs. (4.1)–(4.4)): root mean square error ( $RMSE, m^2 ha^{-1}$ ), relative root mean square error ( $RMSE_{rel}, \%$ ); mean deviation ( $MD, m^2 ha^{-1}$ ); and relative mean deviation ( $MD_{rel}, \%$ ).

$$RMSE = \sqrt{\frac{\sum_{i=1}^n (\hat{y}_i - y_i)^2}{n}} \tag{4.1}$$

$$RMSE_{rel} = 100 \times \frac{RMSE}{\bar{y}} \tag{4.2}$$

$$MD = \frac{1}{n} \sum_{i=1}^n (\hat{y}_i - y_i) \tag{4.3}$$

$$MD_{rel} = 100 \times \frac{MD}{\bar{y}} \tag{4.4}$$

where  $\hat{y}_i, y_i$  and  $\bar{y}$  are the predicted, measured and mean values of total basal area, respectively and  $n$  is the number of observations used for model calibration. Models with good statistical precision and low prediction error were considered for further analysis of volume yield. The quality of the final basal area projection model was studied graphically

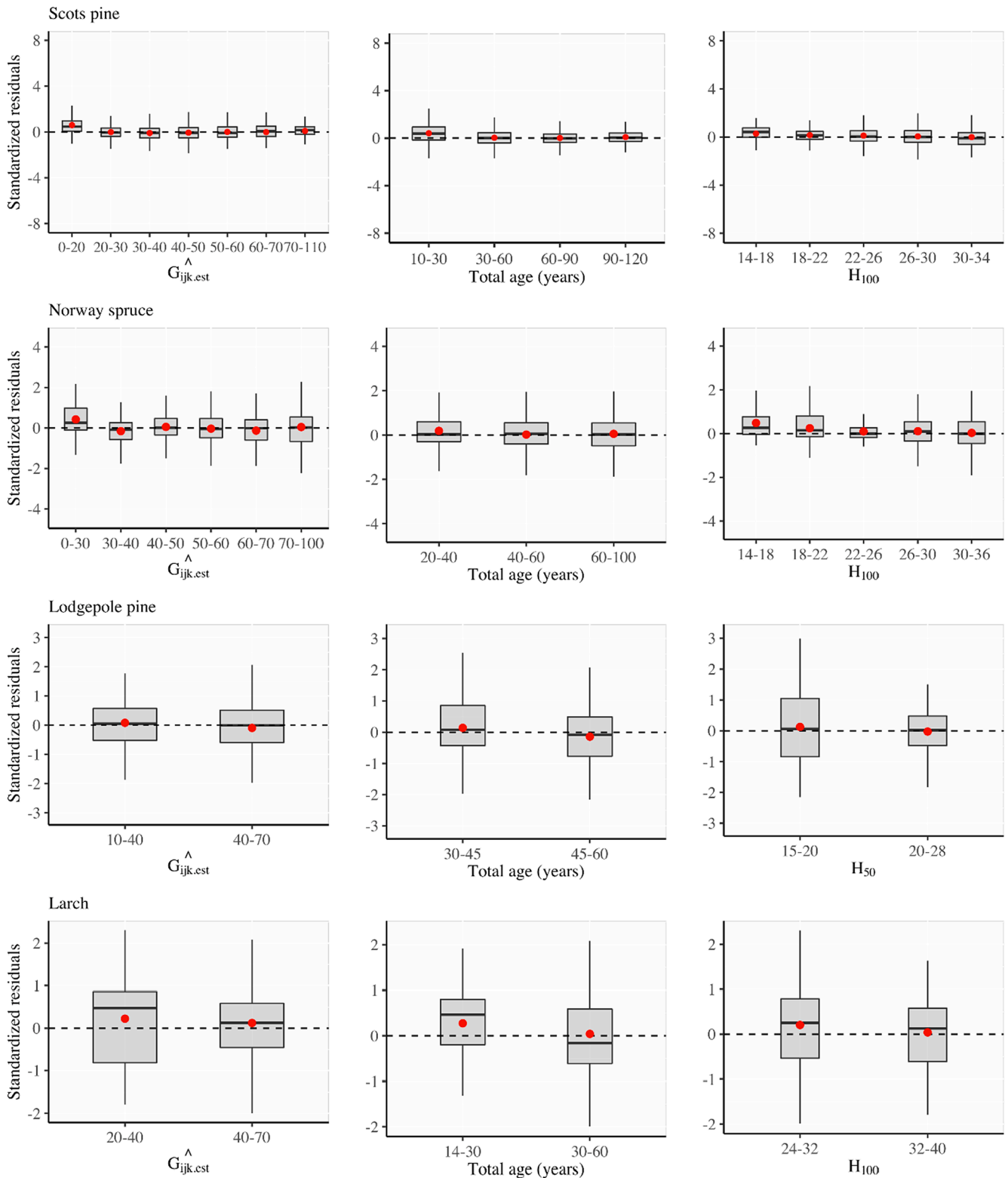


**Fig. 4.** Standardized (Pearson) residuals versus predicted basal area ( $\hat{G}_{ijk}$ ,  $m^2 ha^{-1}$ ), age and site index (m). Site index is expressed as height at 100 years ( $H_{100}$ ) for Scots pine, Norway spruce and Larch, and at 50 years ( $H_{50}$ ) for Lodgepole pine. The red dots are calculated residual means, and horizontal dashed lines denote the expected mean residual ( $[E(\epsilon) = 0]$ ). (For interpretation of the references to colour in this figure legend, the reader is referred to the web version of this article.)

by (1) the distribution of model residuals over plot-level basal area predictions ( $\hat{G}_{ijk}$ ), stand age and SI; and (2) the trajectories of the  $\hat{G}_{ijk}$  curves on the profiles of observed  $G_{ijk}$  for different SI, assuming the growth function passes through current basal area ( $G_{ijl}$ ) at initial mea-

surement age ( $A_{ijl}$ ). Using the fixed-part of the selected model, the expected total basal area productions at ages corresponding to the observed measurement years for each plot were derived. These predictions of basal area were used as predictors to simulate the expected plot-level total volume yield.

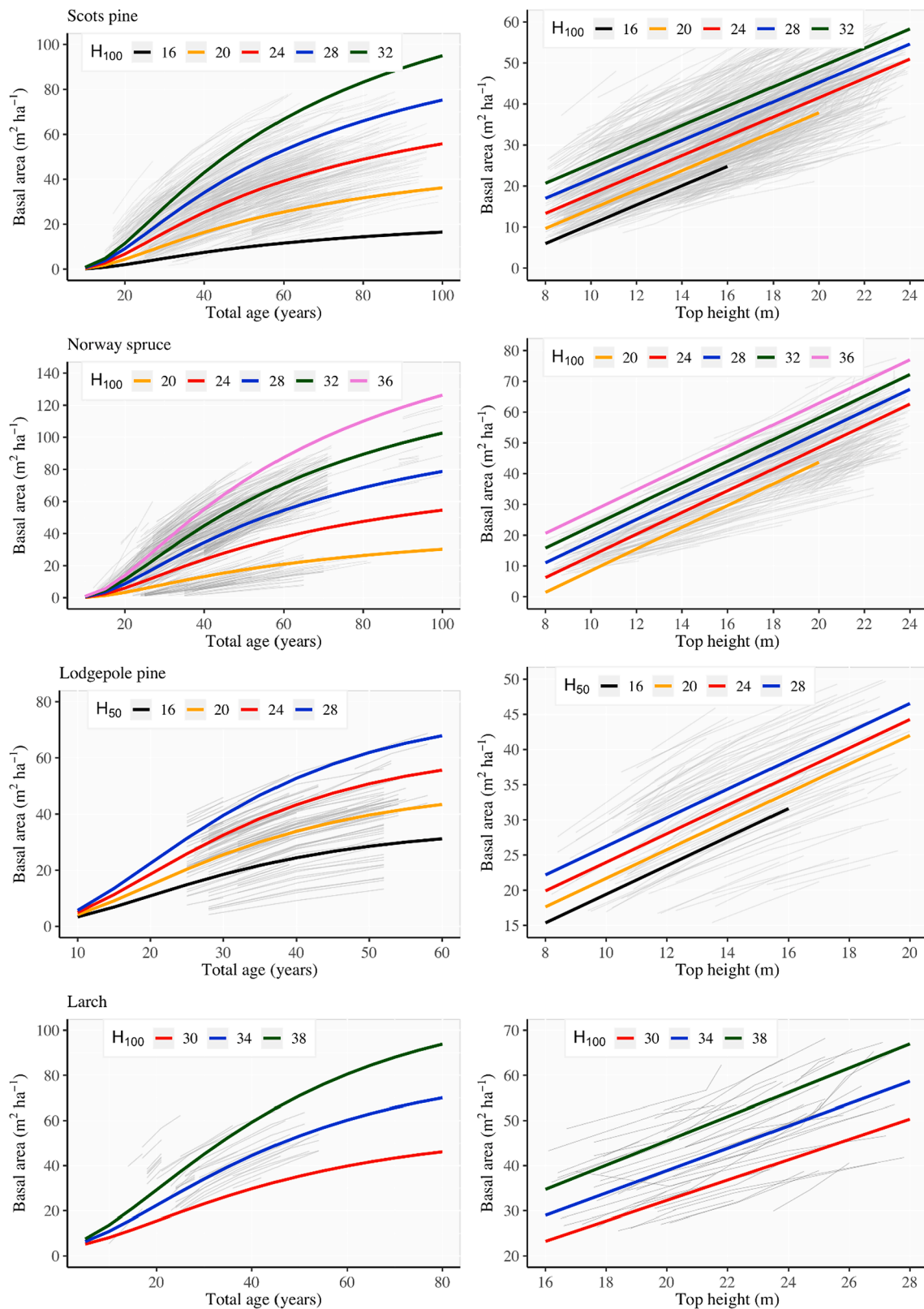
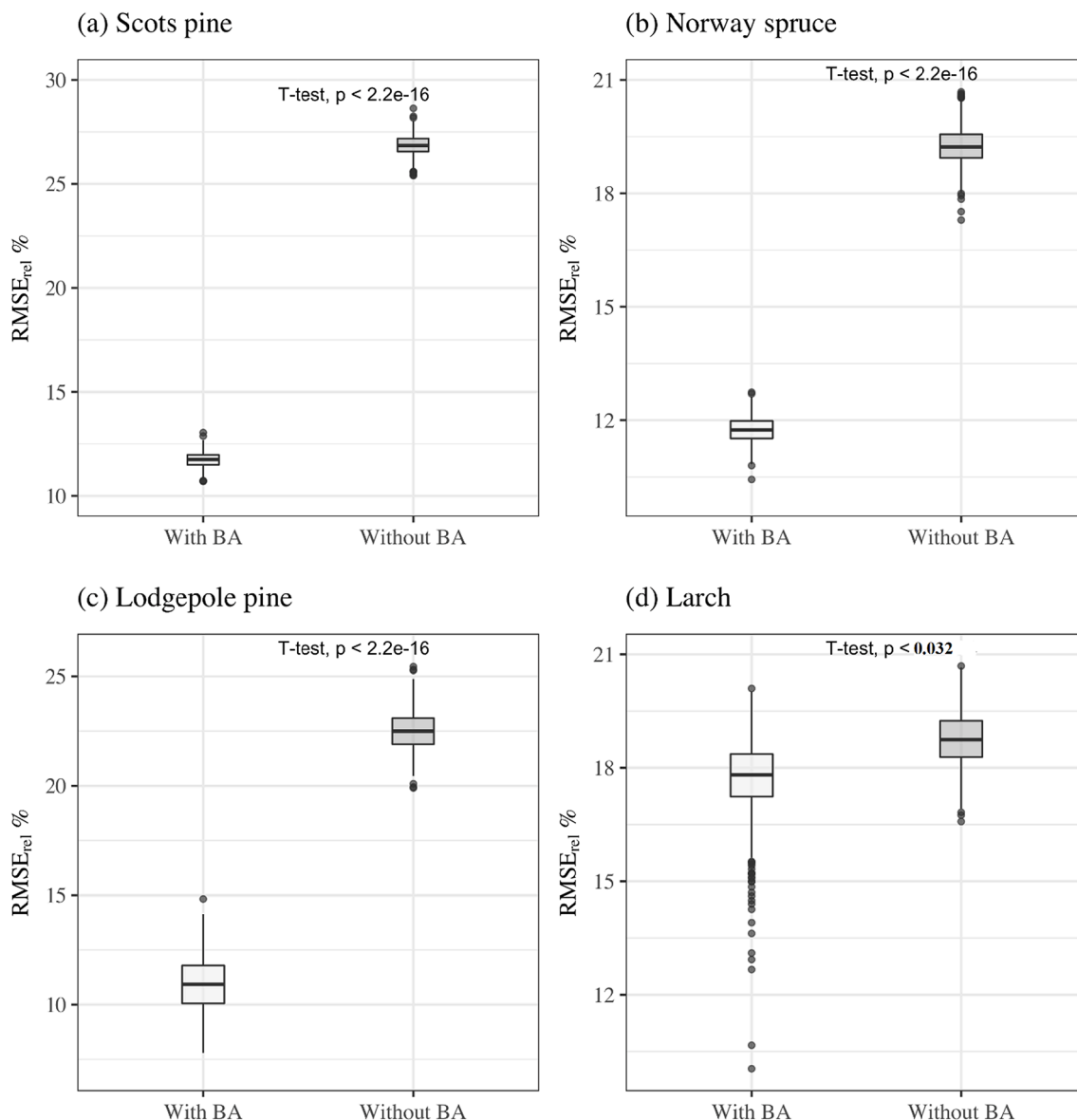


Fig. 5. Left panel: mean predicted basal area over age according to site index; Right panel: Basal area-mean top height relationships. Observed data are shown as solid grey lines.

#### 2.4. Modelling the variations in total volume-top height relationship

To show potential differences in total volume yield (including volumes of removed and dead trees) between sites, the observed volume

yield ( $V$ ) was expressed as an allometric function of mean top height ( $H$ ). However, the volume-height relationship (Eq. (5)) was adjusted with information from total basal area production ( $G$ ), assuming a constant form factor as



**Fig. 6.** Accuracy (relative RMSE, %) of species-specific volume yield equations with or without basal area as a covariate to top height (Eq. (5)). Note the different scales on the y-axis.

$$V = \alpha_0 \times H^{\alpha_1} \times G^{\alpha_2} + \varepsilon \tag{5}$$

where  $\varepsilon$  is randomly distributed errors with a zero mean [ $E(\varepsilon) = 0$ ] and with an unknown constant variance [ $\text{Var}(\varepsilon) = \sigma^2$ ], and  $\alpha$  s are parameters to be estimated.

Variables ( $H$ ) and ( $G$ ) were derived from the height and basal area development functions (see Sections 2.2 and 2.3). Due to the hierarchical structure of the data, Eq. (5) was expressed as a nonlinear mixed-effects time series model to account for both plot and site random variances as:

$$V_{ijk} = \gamma_i + c_{ij} + \alpha_0 \times H_{ijk}^{\alpha_1 + \gamma_i + c_{ij}} \times G_{ijk}^{\alpha_2 + \gamma_i + c_{ij}} + \varepsilon_{ijk} \tag{5.1}$$

where  $V_{ijk}$  is the total volume for plot  $j$  of site  $i$  in year  $k$ ,  $\gamma_i$  and  $c_{ij}$  are the random effects of for site  $i$  and for plot  $j$  of site  $i$ , respectively. Both  $\gamma_i$  and  $c_{ij}$  are independent of  $\varepsilon_{ijk}$  and are normally distributed with mean zero and variances  $\sigma^2_s$  and  $\sigma^2_p$ , respectively [i.e.,  $\gamma_i \sim N(0, \sigma^2_s)$  and  $c_{ij} \sim N(0, \sigma^2_p)$ ].

The random-effects parameters were added sequentially to the fixed-effects parameters until convergence was achieved. The volume-height relationship typically exhibits a curvilinear form with heteroscedastic

variance of the individual model errors ( $\varepsilon_{ijk}$ ) (Haworth and Vincent, 1982; McRoberts and Westfall, 2016). Therefore, the mean of the response variable was modelled with a nonlinear power variance function with three parameters as:

$$V(\varepsilon_{ijk}) = \omega^2 (\delta_0 + |\hat{V}_{ijk}|^{\delta_1})^2 \tag{5.2}$$

The temporal and spatial dependencies among the observations were also modelled using a first order autoregressive covariance structure (see estimator 3.3). The use of predicted values of top height and basal area as explanatory variables in the volume models (Eqs. (5) and (5.1)) has the tendency of propagation of error which could inflate the variances of the estimated model parameters (McRoberts and Westfall, 2016). To check this, non-parametric bootstrap resampling (with replacement) was used to examine the uncertainty associated with the estimated model parameters (Eq. (5.1)). We drew 1000 bootstrapped samples from a population made up of the original sample data. For each bootstrapped replicate, the model parameters were determined and the means of each parameter for the 1000 samples were estimated. The sampling distribution of the estimated model parameters were

**Table 5**  
Parameter estimates of species-specific volume ( $\text{m}^3 \text{ha}^{-1}$ ) yield functions (Eq. (5.1)). Values in parenthesis are estimated standard errors.

| Class                     | Parameter  | Scots pine   | Norway spruce          | Lodgepole pine         | Larch                  |                        |
|---------------------------|--|--|------------------------|------------------------|------------------------|------------------------|
|                           |  | Estimates  |                        |                        |                        |                        |
| Fixed effects             | $\hat{\alpha}_0$   | 0.8013<br>(0.0117)   | 0.7498<br>(0.0196)     | 0.8783<br>(0.0379)     | 1.4005<br>(0.0749)     |                        |
|                           | $\hat{\alpha}_1$   | 1.0208<br>(0.0116)   | 1.1781<br>(0.0215)     | 0.9251<br>(0.0243)     | 1.6359<br>(0.0309)     |                        |
|                           | $\hat{\alpha}_2$   | 0.8062<br>(0.0083)   | 0.7169<br>(0.0149)     | 0.8839<br>(0.018)      | 0.1558<br>(0.0127)     |                        |
|                           | Plot-level random effects  |  |                        |                        |                        |                        |
|                           | $(c_{ij})$   | $\widehat{\text{var}}(\hat{\alpha}_0)$   | 0.0012                 |                        | $1.02 \times 10^{-07}$ | $8.28 \times 10^{-10}$ |
|                           |  | $\widehat{\text{var}}(\hat{\alpha}_1)$<br>$\widehat{\text{var}}(\hat{\alpha}_2)$ |                        | $8.17 \times 10^{-05}$ |                        |                        |
| Site-level random effects |  |  |                        |                        |                        |                        |
| $(\gamma_i)$              | $\widehat{\text{var}}(\hat{\alpha}_0)$<br>$\widehat{\text{var}}(\hat{\alpha}_1)$<br>$\widehat{\text{var}}(\hat{\alpha}_2)$ | 0.0023   |                        | 0.002                  | 0.0172                 |                        |
|                           |  |  | $5.52 \times 10^{-04}$ |                        |                        |                        |
| Residual Variance         |  |  |                        |                        |                        |                        |
| $V(\epsilon_{ijk})$       | $\hat{\omega}^2$<br>$\hat{\delta}_1$<br>$\hat{\delta}_0$   | 1.1546<br>0.4784   | 17.795<br>0.2951       | 2.232<br>0.4749        | 1.883<br>4.0237        |                        |
|                           |  |  | $1.59 \times 10^{-07}$ | $1.34 \times 10^{-04}$ | $1.86 \times 10^{-11}$ |                        |
| Autocorrelation           | $\hat{\rho}$<br>RMSE   | 0.104<br>24.27   | 0.009<br>36.98         | 0.002<br>22.44         | 0.2807<br>54.18        |                        |
| Fit statistics            | RMSE <sub>rel</sub> , %  | 11.74  | 11.75                  | 10.96                  | 17.72                  |                        |
|                           | MD   | -0.1584  | -0.1629                | -0.1283                | 1.1717                 |                        |
|                           | MD <sub>rel</sub> , %  | -0.0765  | -0.0517                | -0.0626                | 0.3834                 |                        |
| $n$                       |  | 4405   | 1789                   | 725                    | 453                    |                        |

visualized graphically using histograms, and the confidence interval (the lower and upper limits of the bootstrapped statistic using the percentile method and 95% confidence level) was considered as an approximate variance in the estimated model parameters. The quality of the volume yield model was assessed graphically by the distribution of residuals over plot-level total volume predictions ( $\hat{V}_{ijk}$ ), total age and SI, and numerically by using the accuracy estimators in Eqs. (4.1)–(4.4) (by changing the response variable from basal area to volume). The accuracy of Eq. (5.1) was also compared with alternative models where basal area was excluded as a covariate of top height.

### 2.5. Relationship between yield capacity and site index

To compute the plot-level mean annual total volume increments (MAI) at each measurement occasion, the predicted volume yields were divided by their corresponding total ages. On each plot and site, the MAI at the time of culmination (or late culmination) was considered as the maximum MAI ( $MAI_{max}$ ), and the plot-level  $MAI_{max}$  values were averaged to estimate the site-level  $MAI_{max}$ . The  $MAI_{max}$  was then used as a proxy for yield capacity because it is related to the potential volume yield attainable on a specific site (Elfving and Nyström, 1996). To determine the functional relationship between SI ( $H_{100}$  or  $H_{50}$ ) and  $MAI_{max}$ , two models with  $MAI_{max}$  as the response variable and SI as a predictor were fitted and compared. Model one (Eq. (6.1)) is an exponential function fitted in R statistical environment through the generalised nonlinear least squares (“gnls”) function.

$$MAI_{max} = \alpha_0 \times \exp^{(\alpha_1 \times SI)} + \epsilon \tag{6.1}$$

For model two (Eq. (6.2)), the relation between  $MAI_{max}$  and SI was

fitted by a second-degree polynomial function. This model was identical to the earlier yield capacity functions developed by Hägglund and Lundmark (1982):

$$MAI_{max} = \alpha_0 + \alpha_1 \times SI + \alpha_2 \times SI^2 + \epsilon \tag{6.2}$$

The accuracy and precision of the fitted yield capacity functions were evaluated using the estimators (Eqs. (4.1) and (4.2)), by changing the response variable from basal area to  $MAI_{max}$ . For each species, the yield capacity estimates from the best model in this study was compared to the earlier estimates from Hägglund and Lundmark (1982). For spruce, additional comparisons were made with Elfving and Nyström (1996) in central-northern Sweden.

## 3. Results

### 3.1. Regression functions for basal area growth prediction

Predicting basal area yield at the end of the growth period as a function of current basal area, initial stand density, site index and total age through nonlinear mixed-effects time series models produced acceptable estimates for the studied tree species. All tested functions converged and model accuracies are presented in Table 3. The largest deviations in relative terms were found for F03 (Levakovic) models, especially for Larch where the error was about 18% of the observed mean. The function F01 (Pienaar et al., 1990) was most suitable for Scots pine and Norway spruce, whereas those of Lodgepole pine and Larch were adequately modelled by the Bertalanffy-Richards function (F04). For these functions (F01 and F04), the relative errors around basal growth predictions were within 2–6%, though they all underestimated the average basal area growth. Nevertheless, in absolute terms, the underestimation of the models was <1% for all species.

For Scots pine, Norway spruce and Lodgepole pine, the estimated fixed-effects parameters were statistically significant at 1% error margin. However, the parameters of age ( $\hat{\alpha}_0$ ) and site index ( $\hat{\alpha}_2$ ) for Larch were not significant ( $p > 0.05$ ) as the estimated standard errors had similar values as the coefficients (Table 4).

As expected, the mixed modelling approach produced variance estimates that were larger between sites than between plots within sites. For Norway and Scots pine, the random slopes of age, site index and initial density enhanced efficient model calibration. For Larch, random age was relevant, whereas site index improved the calibration of random variances of Lodgepole pine. The within-group residual error variances were adequately modelled by the two-parameter power function for Norway spruce and Scots pine, while the three-parameter was suitable for Lodgepole pine and Larch. The estimated first order temporal autocorrelations were also small (0–0.294) for all species (Table 4). The model residuals exhibited constant variance that suggests unbiased predictions of basal area over total age and site index (Fig. 4).

The development of total basal area production according to SI was visualized in Fig. 5. The forms of the curves were statistically and practically acceptable on the observed data for all species. As expected, higher site indices reached larger basal area values quicker than lower site indices for all tree species. To explore the between-site variations in basal area yield levels, an increasing relation was observed between total basal area production and mean top height (Fig. 5).

$\hat{\rho}$  is the estimated first order temporal autocorrelation;  $n$  is the number of observations used for model fitting;  $\widehat{\text{var}}$  is the estimated variance;  $\widehat{\text{cov}}$  is the estimated covariance of parameters.

### 3.2. Regression functions for total volume-top height relationships

To characterize total volume yield and the variations across sites, allometric expressions of volume yield and mean top height were adjusted with information on total basal area production. Addition of basal area improved the volume-height relationships where the relative

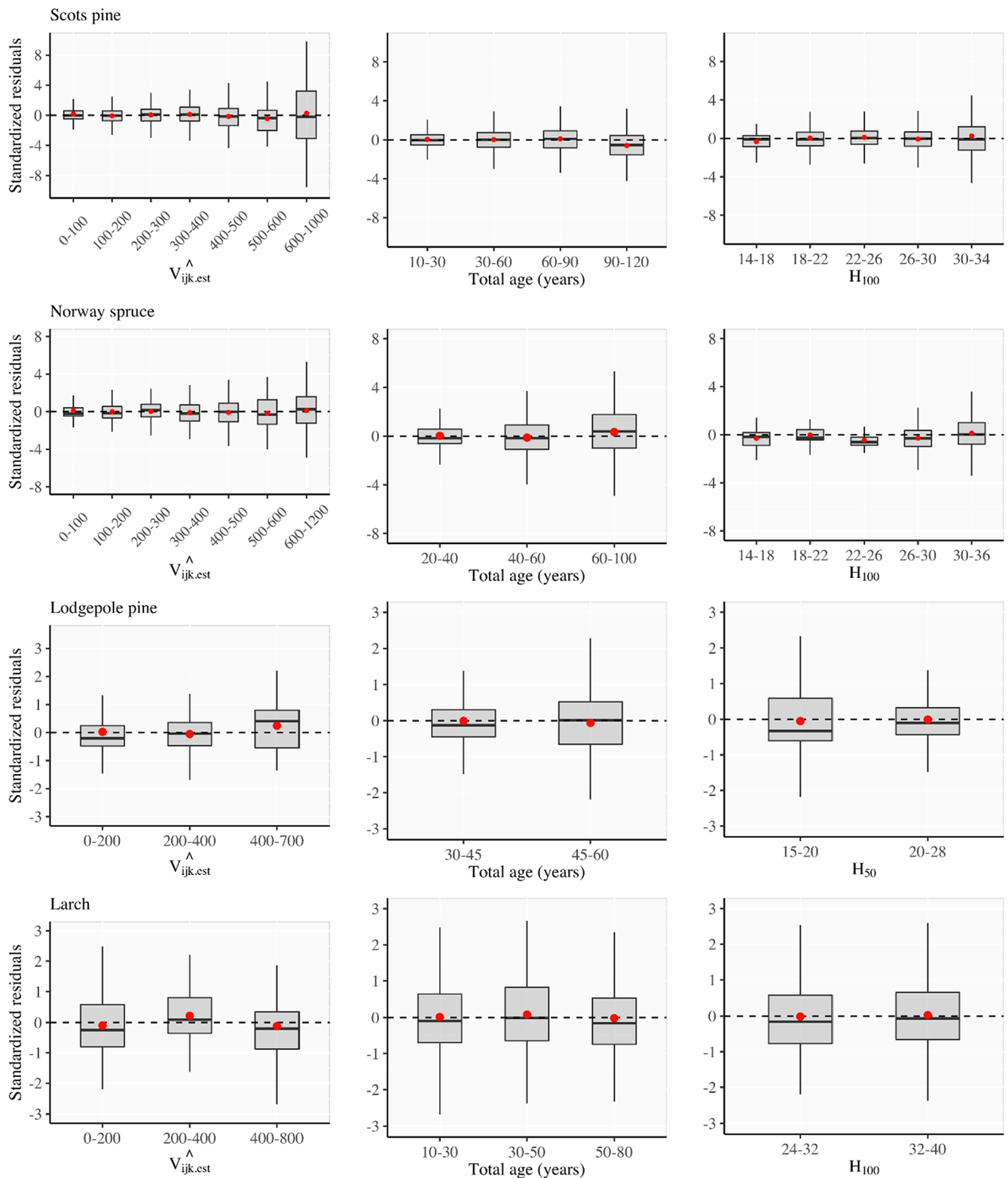
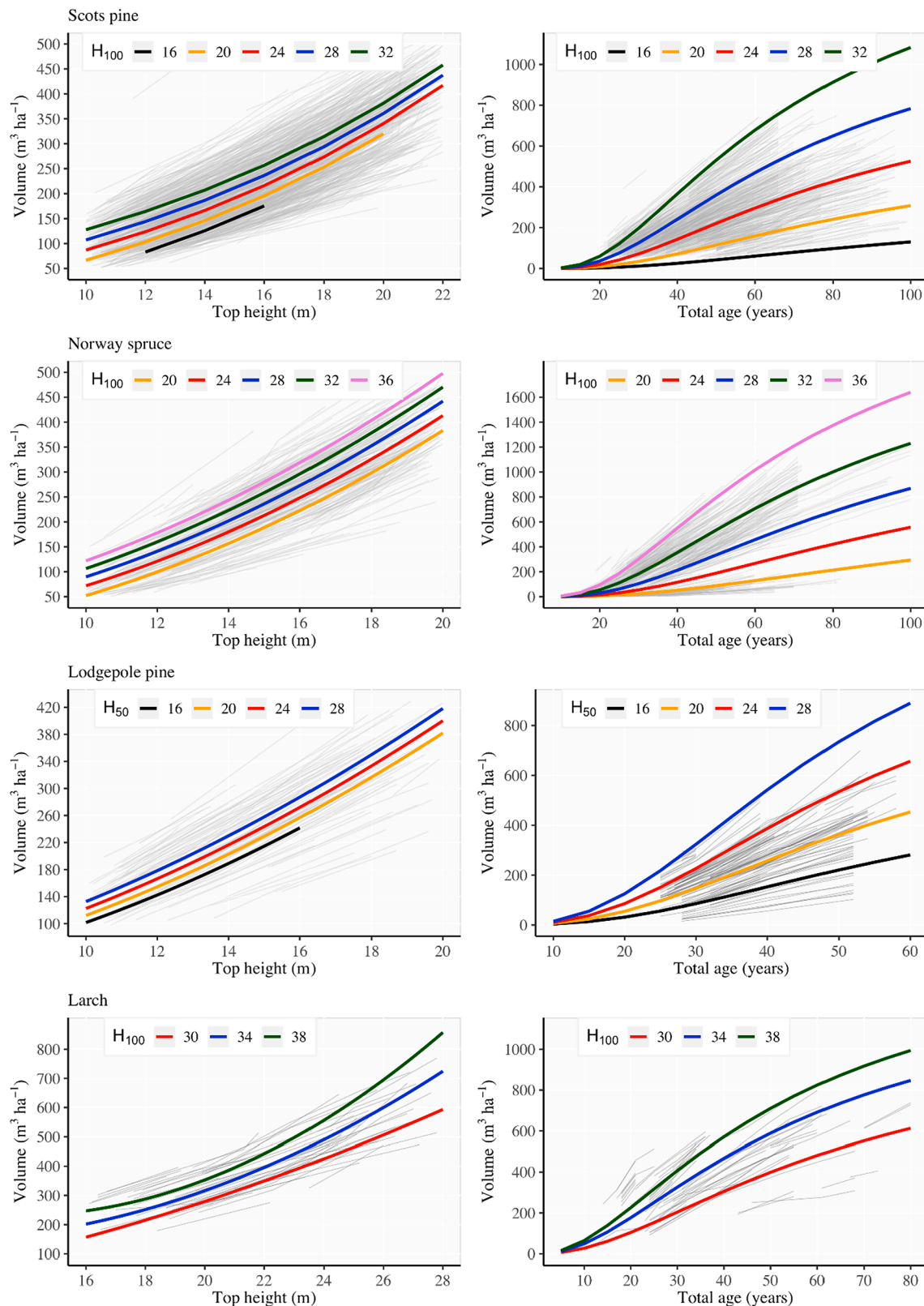


Fig. 7. Standardized (Pearson) residuals versus predicted total volume ( $\hat{V}_{ijk}$ ,  $m^3 ha^{-1}$ ), age and site index (m). Site index is expressed as height at 100 years ( $H_{100}$ ) for Scots pine, Norway spruce and Larch, and at 50 years ( $H_{50}$ ) for Lodgepole pine. The red dots are calculated residual means, and horizontal dashed lines denote the expected mean residual ( $E(\epsilon) = 0$ ). (For interpretation of the references to colour in this figure legend, the reader is referred to the web version of this article.)

model errors were reduced on the average by a factor of 1.5 for all species (Fig. 6).

Table 5 presents the regression summary of the species-specific volume yield equations. The relative errors ( $RMSE_{rel}$ , %) of the species-specific volume yield models were within 10–18% of the mean

values for all species (Table 5). For Larch, the model overestimated the volume yield by 0.4%, whereas those Scots pine, Norway spruce and Lodgepole pine were underestimated on the average by 0.2%. The calibration of plot- and site-level random components adequately captured the variances in volume yields, and the within-group error



**Fig. 8.** Left panel: total volume yield levels (volume-height relationship); Right panel: examples of the development of total volume production over age with a given site index.

variances were efficiently modelled by the power functions. Evaluation of the models' residuals showed variance homogeneity over predicted volume yields, total age and site index (Fig. 7).

$\hat{\rho}$  is the estimated first order temporal autocorrelation;  $n$  is the

number of observations used for model fitting;  $\widehat{var}$  is the estimated variance.

In the volume models, predicted mean top height and basal area were used as predictors, and there is a tendency of error propagation. Un-

**Table 6**

Parameter estimates and fit-statistics of functions relating yield capacity to site index for different tree species. "SE" is estimated standard error.

| Species        | Parameter        | Estimate | SE     | p-value | RMSE (rel, %) | R <sup>2</sup> |
|----------------|------------------|----------|--------|---------|---------------|----------------|
| Scots pine     | $\hat{\alpha}_0$ | 0.4613   | 0.0511 | <0.0001 | 0.9757        | 0.809          |
|                | $\hat{\alpha}_1$ | 0.1006   | 0.0041 | <0.0001 | (16.73)       |                |
| Norway spruce  | $\hat{\alpha}_0$ | 0.5558   | 0.0889 | 0.0037  | 1.047         | 0.904          |
|                | $\hat{\alpha}_1$ | 0.0929   | 0.0049 | <0.0001 | (11.14)       |                |
| Lodgepole pine | $\hat{\alpha}_0$ | 0.8291   | 0.0729 | <0.0001 | 0.436         | 0.956          |
|                | $\hat{\alpha}_1$ | 0.1038   | 0.0039 | <0.0001 | (5.52)        |                |
| Larch          | $\hat{\alpha}_0$ | 0.9583   | 0.1547 | <0.0001 | 1.164         | 0.876          |
|                | $\hat{\alpha}_1$ | 0.0695   | 0.0044 | <0.0001 | (10.82)       |                |

certainty analyses of the parameter estimates were conducted by bootstrap resampling. The estimated model parameters occurred within the interval from the 2.5th to the 97.5th confidence limits, indicating no apparent systematic effects of error propagation in all species, except for Larch, which showed large uncertainty in the estimated model parameters ( $\hat{\alpha}_1$  and  $\hat{\alpha}_2$ ) (Fig. A.1, appendix). This might be due to the combined dataset for the two Larch species for modelling since we had very few observations for either species. However, the two species have different growth rates (Siberian Larch has slower growth rate than European Larch) which could introduce additional uncertainty. Despite this limitation, a larger part of the sampling distribution of estimated parameters were within the acceptable error bounds (Fig. A.1, appendix).

The volume production at a given top height is shown in Fig. 8. As expected, the volume yield levels showed increasing relationships, suggesting site-dependent variations in volume-height trajectories (Fig. 8, left panel). Thus, larger volume yields are attained at higher SIs (Fig. 8) and the culmination in mean and current annual volume increments is earlier than for lower SIs (Fig. A.2, appendix). The observed volume-height trajectories follow the same order as the basal area yield levels (Fig. 5) for all species. This offers support to the assertion that given the same mean top height, the volume yield levels would be different between sites if the basal area production levels are also different.

### 3.3. Functional relationship between site index and yield capacity

The relationship between yield capacity and SI was best fitted by the exponential regression function (Eq. (6.1)) for the studied tree species. Information on model parameter estimates and goodness-of-fit statistics are given in Table 6. Generally, SI was significant in predicting yield capacity and the form of the curves described by the models was statistically and practically acceptable (Fig. 9). The explained variation (adjusted R<sup>2</sup>) ranged from 80 to 96% and the relative model errors ranged from 6 to 17%, with Scots pine and Norway spruce showing the largest variations around the observed mean.

In Fig. 10, the yield capacities predicted from the present study were compared to earlier estimates from Hägglund and Lundmark (1982). For Scots and Norway spruce, significant differences were observed at both lower and higher SIs. At lower SIs, the estimated yield capacities from the current study were smaller than the predictions by Hägglund and Lundmark (1982) and vice versa at higher SIs. For Norway spruce, predicted yield capacity was similar to Elfving and Nyström (1996) in central-northern Sweden. For Lodgepole pine, the estimates were similar at lower SI, but differed markedly at higher SI classes between the functions.

## 4. Discussion

The purpose of this study was to develop functional relationships

between yield capacity and site index (SI) for the major tree species in Swedish boreal forests. The newly developed yield capacity functions were also compared with earlier functions made for the studied species. This was approached by utilizing measured tree growth data from long-term experiments (LTEs). The observations covered almost the entire rotation periods and a wide range of site fertility gradients that represent managed forests in Sweden. Thus, in this study, the LTE data were assumed as valid growth references for yield capacity estimation.

Height and basal area are key variables in the empirical growth models used in Sweden, for example in the Heureka planning system. While height is the dependent variable during the establishment stage (mean height < 7 m), basal area drives the growth models for established stands (Elfving, 2010b; Wikström et al., 2011). As such, their estimations are crucial for evaluation of forest yield capacity (Elfving and Nyström, 1996; Burkhardt and Tomé, 2012). Height growth models were not developed in the current study, but instead, the observed top heights were used for SI estimation with existing height development functions, which when combined with initial stand density, produced accurate and reliable estimates of basal area production over time (Table 4, Fig. 4). This follows earlier reports on the influence of initial spacing and site quality on the asymptotic basal area growth of even-aged stands (Pienaar and Shiver, 1986; Pettersson, 1992; Elfving, 2010a; Hall et al., 2019). Expressions for basal area often include mean top height and or mean height (Elfving and Nyström, 1996; Hall et al., 2019) but such expressions were avoided in our basal area development functions because top height was later used as a predictor in the total volume estimations. The basal area functions developed in this study show lower residual variations than the current stand-level basal area growth models for Scots pine and Norway spruce in the Heureka system (RMSE m<sup>2</sup> ha<sup>-1</sup>: 1.03 vs. 2.32) but, the conditions for the estimations differ. In the Heureka case, basal area growth is estimated at 5-year periods (Elfving, 2010b; Fahlvik et al., 2014), whereas in our study, the development of total basal area production (yield) is modelled.

The observed increasing relation between total basal area production and mean top height describe the concept of carrying capacity in forest stands (Fig. 5). Usually, "natural basal area" is used to describe the maximum basal area production for un-thinned stands (e.g. Assmann, 1961; Hasenauer et al., 1994), however, we modelled the total basal area production (including dead, ingrowth trees etc.) for each site and the observations spanned across plots with many measurements before and after first thinnings. In addition, the thinning interventions were mainly of thinning-from-below. Thus, our basal area estimates can potentially describe the productivity differences in relation to site index. This was supported by Eq. (5) and Figs. 6 and 8. Errors in the volume-height relations were significantly reduced by a factor of 1.5 units when including basal area (Fig. 6) and the yield level trajectory was higher for high site index (Fig. 8). A similar study by Ung and Ouellet (1991) found an improved estimation of total volume (11–12% error) from both top height and basal area per hectare for black spruce (*Picea mariana* (Mill.)) stands in the Boreal Forest Region of Lebel-sur-

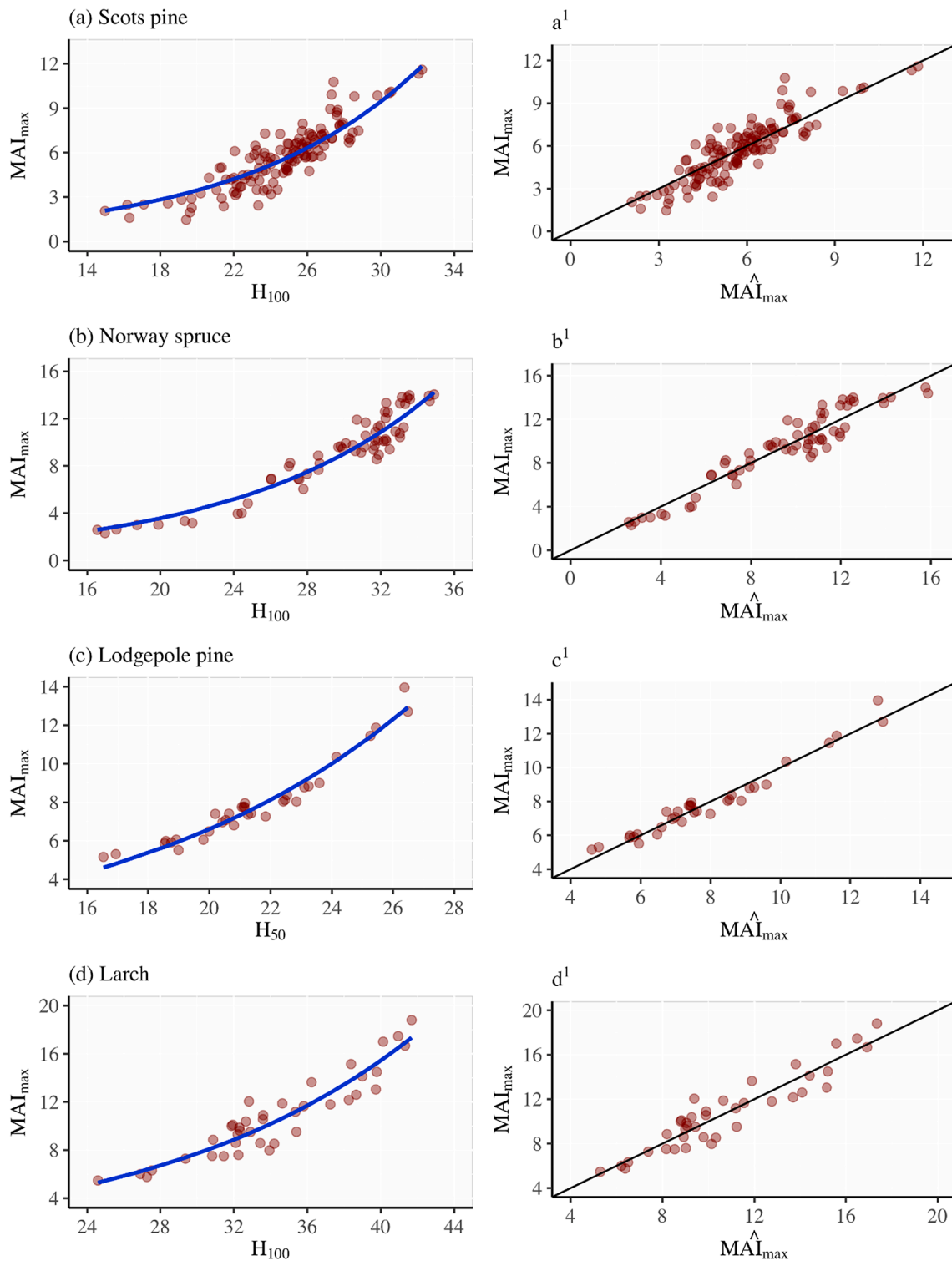


**Fig. 9.** Relationship between yield capacity ( $MAI_{max}$ ,  $m^3 ha^{-1} yr^{-1}$ ) and site index (expressed as height (m) at 100 years ( $H_{100}$ ) for Scots pine, Norway spruce and Larch, and at 50 years ( $H_{50}$ ) for Lodgepole pine). Right panels show 1:1 relationship between the observed (obtained from measured total volume yield and age) and predicted yield capacity.

Quévillon, Canada. In other studies of growth-density relationships, [Allen et al. \(2020\)](#) also found that gross volume increment increased with increasing basal area for Norway spruce plantations in Norway. Our results follow closely Assmann’s yield level investigation of Norway spruce, where differences in stands’ common yield levels (total yield at a certain top height) and special yield levels (reaching this certain top height in a particular age) were attributed to differences in basal area

levels given the same initial spacing and treatment ([Assmann 1955](#)). [Schmidt \(1973\)](#) also found that yield level variations in Scots pine is not only site index dependent, but it is also dependent on the basal area development for a given age and top height. Generally, basal area differences at a given top height and age result from the variations of number of stems per hectare and the quadratic mean diameter at breast height (QMD). At the same QMD but differing stand density, different

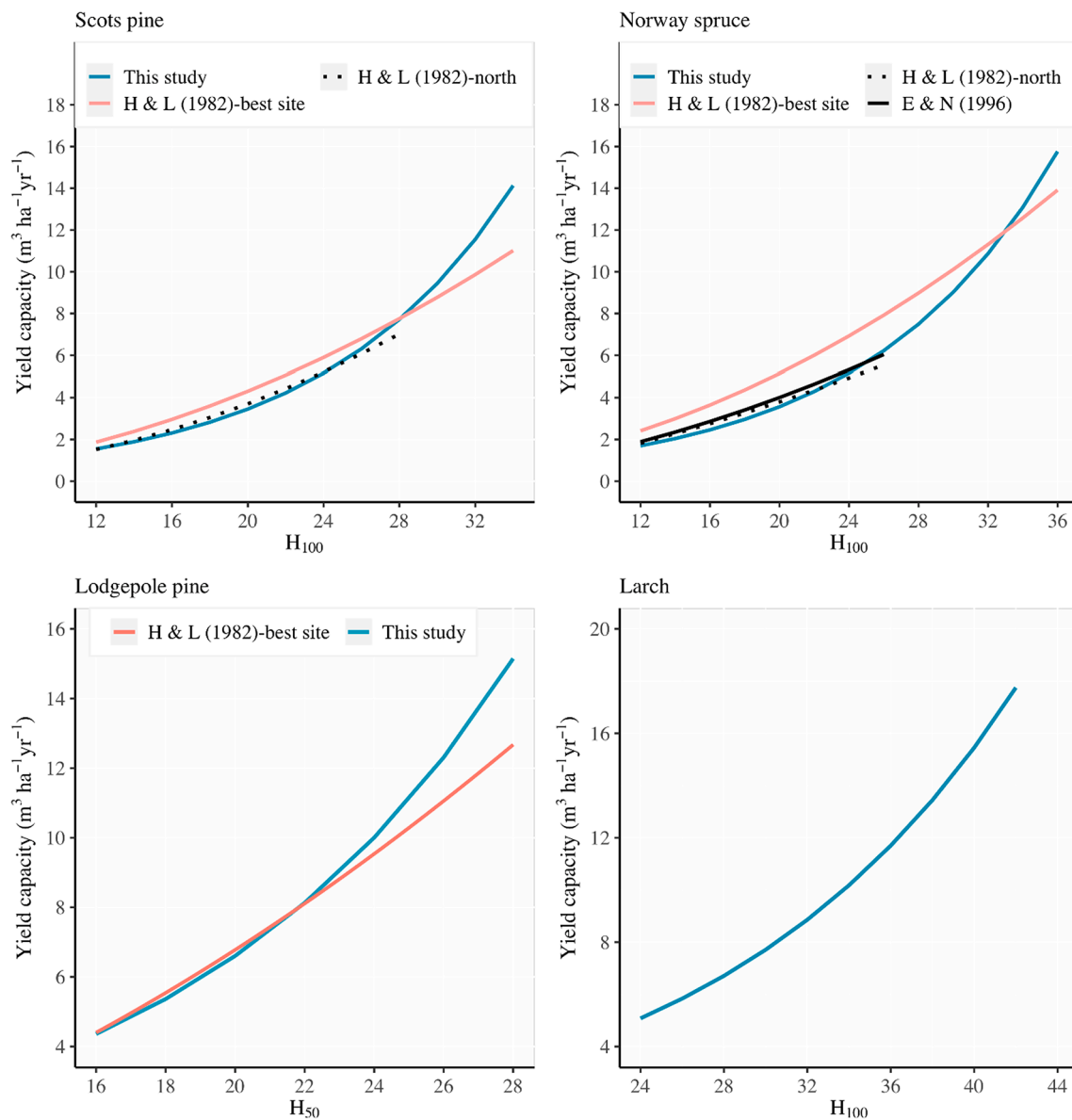


**Fig. 10.** Predicted mean yield capacity from current (denoted as “This study”) and previous studies (Hägglund and Lundmark (1982) denoted as [H&L (1982); Elfving and Nyström (1996) denoted as E&N (1996)]. H&L (1982)-best site refers to lingonberry-sites for pine stands (below 200 m above sea level) and blueberry-sites for spruce over the whole country. H&L (1982)-north refers to pines (above 200 m above sea level) and spruces (poor sites) in northern Sweden. E&N (1996) refers to spruce sites in central-northern Sweden. Note that for Larch no previous model is available for comparison. Extrapolations are made beyond the observed SI ranges (see Table 1).

yield levels are observed using the relative space system. Different QMDs at the same stem number also allude to differences in taper and yield levels. For example, Hasenauer et al. (1994) found that differences in volume yield levels of Loblolly pine across the physiographic regions in southern United States were largely explained by differences in maximum basal area development, which was in turn supported by the sites' potential number of stems per unit area at a given top height. This suggests that, the Eichhorn's law is exclusively rapid for total volume estimation, but augmenting the volume-top height relationship with basal area guarantees high accuracy in yield level estimation (Bontemps and Bouriaud, 2014). Other reasons such as changes in stem form may have effects on the volume growth, but this was assumed to have very little influence in the present study.

Yield capacity was positively correlated with SI for all studied tree species and the exponential model adequately described the functional forms of the relationship (Fig. 9 and Table 6). The developed yield capacity functions from the current study were compared to earlier

functions by Hägglund and Lundmark (1982) and significant differences were observed (Fig. 10). Two possible explanations pertaining to (1) the data origin and method of estimation and (2) environmental changes could be given for the observed differences.

The material (data) used for constructing SI functions differed in this study and that of Hägglund and Lundmark (1982). In the latter, the calibration data were from felled-sectioned trees (in temporary plots) growing in the 1940's with an average age at breast height of about 70 years. Thus, the data mostly represented tree development conditions at the first half of the 20th century. The site indices were estimated by functions constructed from static- and fixed-base age equation of Chapman-Richard (Hägglund, 1972, 1973, 1974). However, in the current study, the SI functions (Elfving and Kiviste, 1997; Elfving, 2009; Liziniewicz et al., 2016) used were derived from difference equations that were parameterised with repeated sample plot data from homogeneous stands (even-aged monocultures) in the LTEs, and the data mainly reflected growth in the second half of the 20th century up to 1990. The

difference equations have shown better performance in SI estimation for several studies than their static counterparts (e.g. Cieszewski and Bailey, 2000; Nord-Larsen et al., 2009). Currently, the new SI functions demonstrate a change in the growth form and they adequately describe the growing conditions of Swedish forests. For example, in Scots pine stands; the new SI functions are indicating about 2 m increase in the height growth compared to older SI functions (Elfving and Kiviste, 1997). Thus, there is a potential bias if yield capacity is based on older SI functions. In a similar study, Elfving and Nyström (1996) observed that the yield capacity for new generation of Norway spruce plantations in northern Sweden is underestimated (by ~35%) if the site quality estimation is based on height and age in old-growth stands.

On the methods of yield capacity estimation, existing growth functions were used to simulate the yield capacities from NFI data collected using temporary sample plots in the early 1980s (Hägglund, 1981; Hägglund and Lundmark, 1982; Ekö, 1985). The Swedish NFI is a statistically distributed sample and so therefore covers a wider amplitude of stand variation (Fridman et al., 2014). Thus, there is the tendency of including stands that are more heterogeneous as well as sites that naturally do not represent the species' distribution. This could potentially affect the growth trajectories during simulation. In addition, with data from the NFI, information on stand history such as provenances is generally unknown and silvicultural treatments (e.g. fertilisation) are mostly uncertain. For instance, in older stands that are naturally regenerated, the site-specific maximum height is mostly affected by early suppression and it would be a misrepresentation when top height is used as an indicator for site quality assessment in such stands (Elfving and Nyström, 1996; Elfving and Kiviste, 1997). Thus, it is not clear whether the NFI data adequately described the growth trajectories in Hägglund and Lundmark (1982). In contrast, this study made use of data from the LTEs where the total volume yield has accumulated and tree growth trajectories can be reliably estimated. It is important to note that Hägglund and Lundmark (1982) stratified their yield capacity functions based on latitude, altitude and forest type described by vegetation classes. However, comparisons were made with the functions that represent the whole country as well as those that describe higher site quality. For Norway spruce and Scots pine, the larger difference (Fig. 10) in the estimated yield capacities is difficult to explain. For Norway spruce, the difference might be due to overestimation of basal area at a given top height (Table S1, appendix). For spruce plantations in central-northern Sweden (62–65°N), for example, at 10 m top height, our function gives on the average the same basal area levels as that of Elfving and Nyström (1996), but the estimates according to (Hägglund, 1981) was about 60% higher than observed. Such higher initial levels of basal area could largely influence the relation between yield capacity and SI as shown by Elfving and Nyström (1996). Other reasons may be attributable to selection effects and low stocking. For instance, there were fewer observations (LTEs) in the lower SIs of Norway spruce at northern Sweden. In addition, these plot had lower levels of stocking, suggesting many small trees in the diameter distribution, which eventually leads to a lower stem-wood volume production (e.g. Nilsson et al., 2012). Nevertheless, our yield capacity estimates for spruce in northern Sweden was on the average similar to Hägglund and Lundmark (1982), when comparisons are made with the northern-specific function. For Lodgepole pine, the estimated yield capacities were similar on lower SIs, but differed markedly on higher SIs (Fig. 10).

Other reasons such as altered site properties by changes in environmental conditions may have also contributed to the observed deviations in the two yield capacity functions. For boreal forests of northern Europe, recent years' growing season temperature and precipitation, atmospheric CO<sub>2</sub> fertilization and nitrogen deposition have improved tree growth and current stands seem to sustain higher stand densities (e.g. Sharma et al., 2012; Kauppi et al., 2014; Henttonen et al.,

2017; Appiah Mensah et al., 2021; Mäkinen et al., 2021). Similarly, effects from improved silviculture and changes in forest management have also contributed to the increased tree growth (Elfving and Teghammar, 1996).

Another important comment to highlight is the validity of the total basal area development, stem volume production and yield capacity functions developed in the current study. We used all tree growth observations during the model fitting to provide robust and confident parameter estimation. To validate the models, independent dataset from LTEs in northern and southern Sweden were used. Higher accuracies similar to levels obtained during model calibration (Tables 3 and 5) were observed for the test data (Fig. A.3, appendix).

## 5. Conclusion

This study highlights the unique contribution of LTEs for evaluating forest site productivity of major forest tree species in boreal Sweden. These observational plots have the capacity to support studies on the health and climate change mitigation potential of boreal forests in northern Europe. The developed functions for total basal area development and total volume production indicated statistical and practical acceptability on both calibration and validation datasets. The total basal area production as a proxy for stands' carrying capacity explained largely the site variations in total volume yield levels. The developed yield capacity functions adequately described stand productivities. Compared with Hägglund and Lundmark (1982), we found differences in the estimated yield capacities on both lower and higher site indices, particularly for the two dominant coniferous species, Scots pine and Norway spruce. For Lodgepole pine, the old functions generally underestimated the yield capacities on higher site indices, but fairly agreed with our estimates on lower site indices. The yield capacity functions from this study describe well the site productivity in the current climate, and are suitable for growth and yield assessment of even-aged (monocultures) Swedish forests. It was not possible to compare the tree species' productions in this study given that the data material for each species was from different locations. However, the functions can later be used for selection and comparison of tree species' production in similar site and management regimes in Sweden.

### *CRedit authorship contribution statement*

**Alex Appiah Mensah:** Conceptualization, Methodology, Data curation, Formal analysis, Writing – original draft, Writing – review & editing. **Emma Holmström:** Conceptualization, Methodology, Writing – review & editing, Supervision. **Kenneth Nyström:** Methodology, Writing – review & editing. **Urban Nilsson:** Conceptualization, Methodology, Data curation, Writing – review & editing, Supervision.

### **Declaration of Competing Interest**

The authors declare that they have no known competing financial interests or personal relationships that could have appeared to influence the work reported in this paper.

### **Acknowledgement**

Special thanks go to Professor (emeritus) Björn Elfving and Dr. Hans Petersson for comments on the earlier manuscript. The Unit of Field Based Research is duly acknowledged for the continuous inventory of observational plots in the LTEs. We thank the two anonymous reviewers for the constructive comments on the initial manuscript. The financial support from the Department of Forest Resource Management to the first author's doctoral studies is greatly acknowledged.

Appendix

Uncertainty in estimated volume model parameters

The uncertainty around the volume parameter estimates using predicted mean top height and basal area as explanatory variables was investigated by bootstrap resampling. We drew 1000 bootstrapped samples from a population made up of the original sample data. For each bootstrapped replicate, the model parameters were determined and the means of each parameter for the 1000 samples were estimated. Sampling distribution of the estimated model parameters were visualized graphically using histograms, and the confidence interval (2.5th and 97.5th limits of the bootstrapped statistic using the percentile method) was considered as approximate variance in the estimated model parameters. No systematic propagation of errors was observed (Fig. A.1).

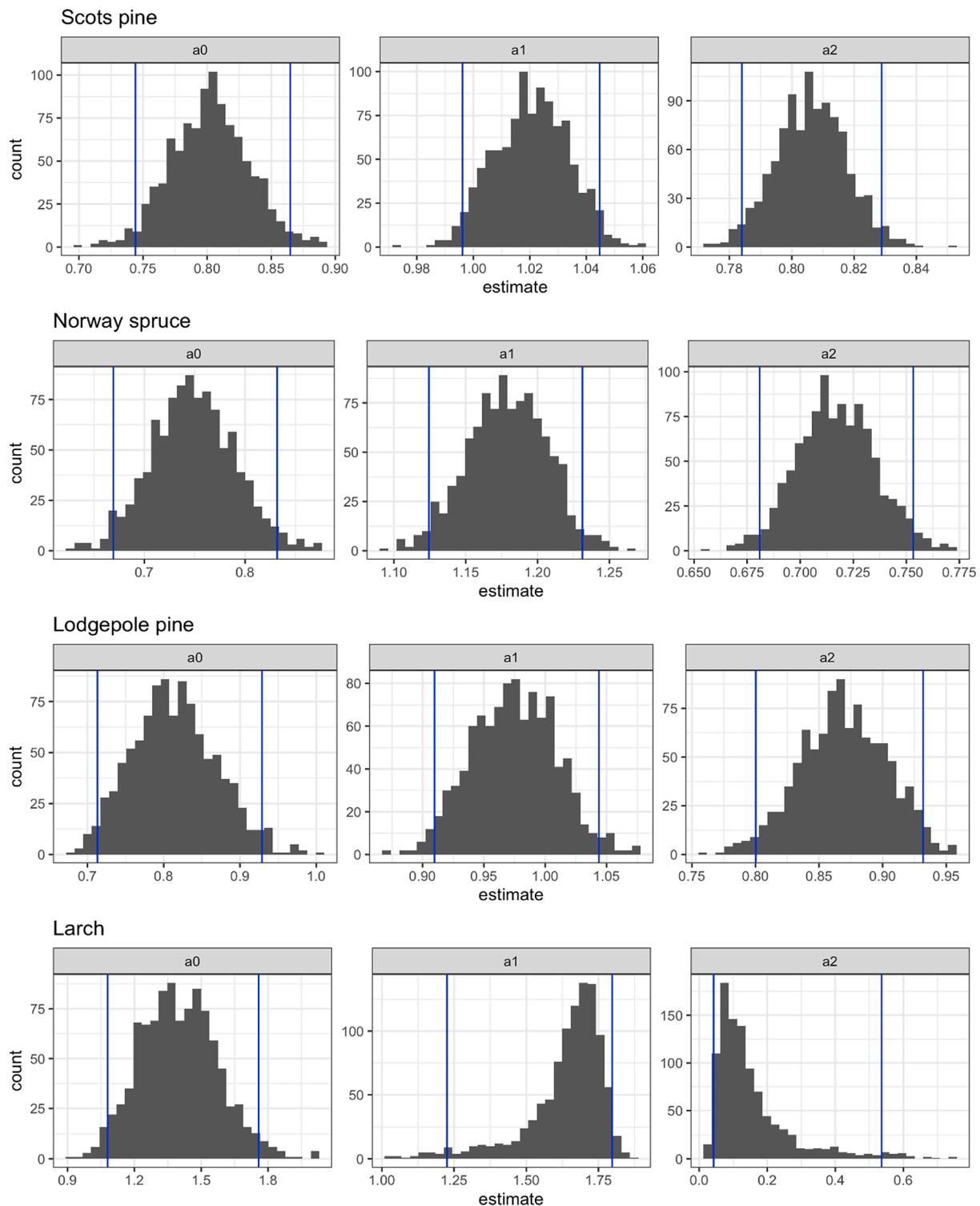


Fig. A.1. Sampling distribution of estimated volume parameters from 1000 bootstrap resamples. The vertical lines show the 2.5th and 97.5th intervals around the bootstrap estimate at 95% confidence level. See Eq. (5) for the definition of model parameters.

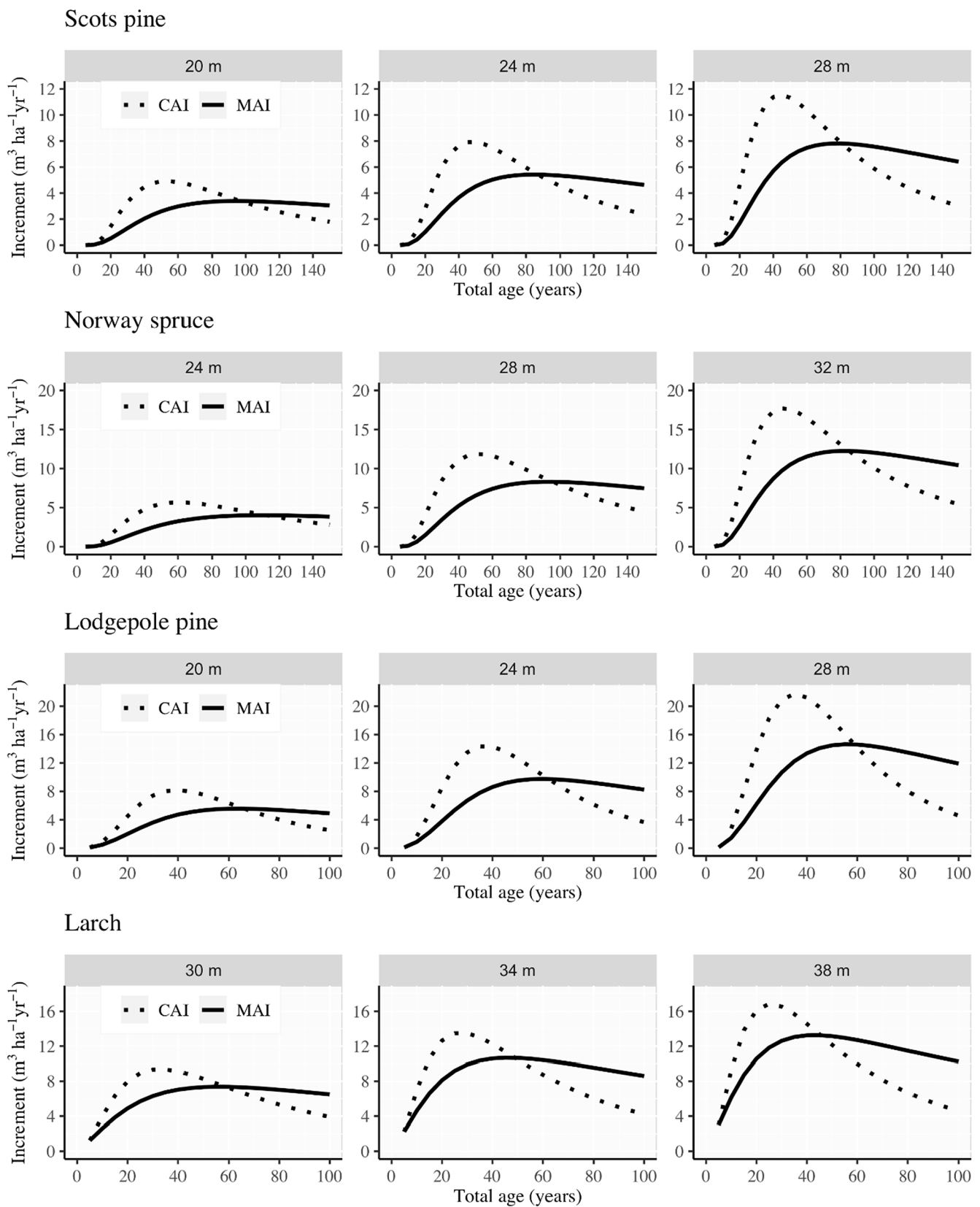


Fig. A.2. Predicted mean (MAI) and current (CAI) annual volume increments for different site indices and species according to the basal area and volume functions developed in this study.

**Table S1**

Observed and predicted mean basal area ( $m^2 ha^{-1}$ ) in different classes of top height. Comparison with earlier studies for Norway spruce at central-northern Sweden (62–65°N).

| Data/function   | Top height (m) |            |            |            |             | Total Mean (SD) |
|-----------------|----------------|------------|------------|------------|-------------|-----------------|
|                 | ≤8.4           | 8.5–9.4    | 9.5–10.4   | 10.5–11.4  | ≥11.5       |                 |
|                 | Mean (SD)      | Mean (SD)  | Mean (SD)  | Mean (SD)  | Mean (SD)   |                 |
| $G_{ijk}$       | 4.5 (2.9)      | 10.9 (3.2) | 15.8 (6.8) | 18.9 (3.5) | 39.2 (23.9) | 22.6 (10.1)     |
| $\hat{G}_{ijk}$ | 3.6 (3.0)      | 10.5 (3.4) | 14.4 (7.3) | 18.6 (7.3) | 39.1 (26.4) | 22.1 (11.3)     |
| EN96            | 10.9 (3.5)     | 12.9 (4.8) | 12.6 (3.5) | 15.3 (6.9) | 17.9 (10.7) | 14.2 (6.7)      |
| H81             | 14.5 (0.8)     | 16.5 (1.0) | 19.4 (0.9) | 22.6 (1.0) | 26.8 (2.7)  | 20.5 (3.9)      |
| $n$             | 25             | 3          | 6          | 6          | 35          | 75              |

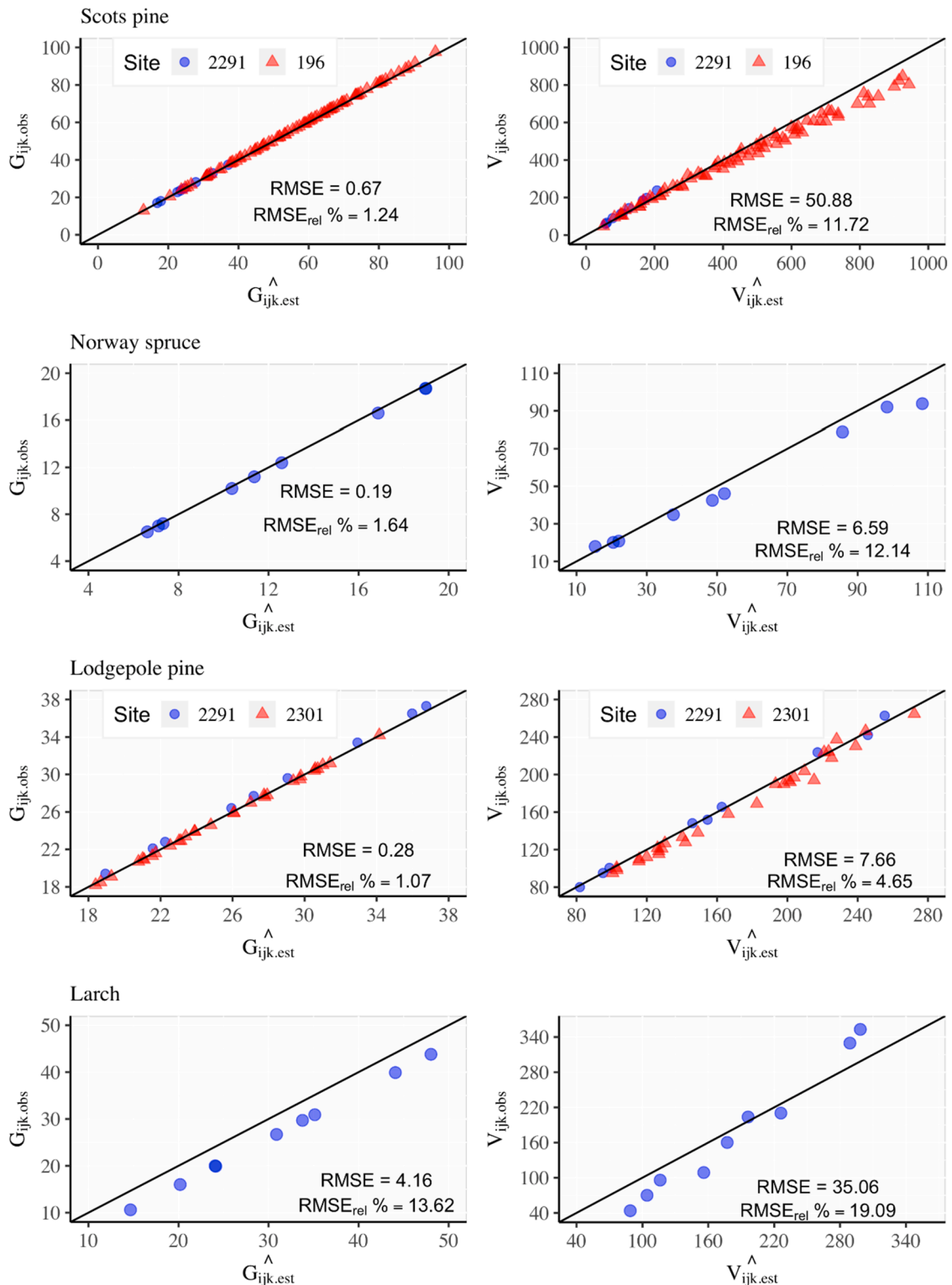


Fig. A.3. Validation of the species-specific basal area and volume ( $\text{m}^3 \text{ha}^{-1}$ ) functions (Tables 4 and 5) on independent data from three sites in Sweden (northern Sweden- latitude  $64^\circ\text{N}$ , southern Sweden- latitude  $58^\circ\text{N}$ ).  $G_{ijk,obs}$  is observed total basal area ( $\text{m}^2 \text{ha}^{-1}$ );  $\hat{G}_{ijk,est}$  is predicted total basal area ( $\text{m}^2 \text{ha}^{-1}$ );  $V_{ijk,obs}$  is observed total volume ( $\text{m}^3 \text{ha}^{-1}$ );  $\hat{V}_{ijk,est}$  is predicted total volume ( $\text{m}^3 \text{ha}^{-1}$ ).

$G_{ijk}$  is observed basal area;  $\hat{G}_{ijk}$  is basal area according to functions (F01 and F04) in the present study (Tables 2 and 4); H81 is basal area according to Hägglund (1981); EN96 is basal area according to Elfving and Nyström (1996);  $n$  is number of observations; SD is standard deviation. Note that the conditions for basal area estimations differed among the functions.

### Model validation on independent data

The basal area and volume functions developed in the present study (Tables 2, 4 and 5) were validated using independent dataset from LTE sites in northern and southern Sweden. The northern sites were located at latitude  $64^\circ\text{N}$  and an altitudinal range of 250–300 m above sea level (a.s.l.). Site 2291 is a tree species trial established in 1992 involving spruce, pine, Lodgepole pine, larch and other exotic species. So far, three inventories have been conducted at 5-year intervals: 2009 (at total age of 19 years), 2014 (at total age of 23 years) and 2019 (at total age of 29 years). The SIs for the tree species were: spruce, 30 m at 100 years; scots pine, 29 m at 100 years; Lodgepole pine, 26 m at 50 years and larch, 33 m at 100 years. Site 2301 is a spacing trial of Lodgepole pine established in the year 1982. First measurement was done in 2011 at 31 years old and the last measurement was in the year 2020 at a total age of 40 years. The SI at latest remeasurement is 20 m at 50 years. The southern site (196) is a Scots pine thinning and yield experiment located at latitude  $58^\circ\text{N}$  and an altitude of 120 m (a.s.l.). The experiments were established at 1931 and first measurements conducted within the same year when the stands were 26 years old. The measurement period is on average 5 years interval and the last measurement was done in 2008 at 102 years. The SI is 28 m at 100 years.

### References

- Allen, M., Brunner, A., Antón-Fernández, C., Astrup, R., 2020. The relationship between volume increment and stand density in Norway spruce plantations. *Forest.: Int. J. Forest Res.* cpaa020. <https://doi.org/10.1093/forestry/cpaa020>.
- Appiah Mensah, A., Holmström, E., Petersson, H., Nyström, K., Mason, E.G., Nilsson, U., 2021. The millennium shift: Investigating the relationship between environment and growth trends of Norway spruce and Scots pine in northern Europe. *For. Ecol. Manage.* 481, 118727. <https://doi.org/10.1016/j.foreco.2020.118727>.
- Assmann, E., 1970. *The principles of forest yield study*. Pergamon Press, Oxford, New York, pp. 506.
- Assmann, E., 1966. Die Schätzung jetziger und künftiger Ertragsleistungen. *Forstw. Centralblatt* 85 (11-12), 355–371.
- Assmann, E., 1961. *Waldertragskunde* [Forest yield science]. BLV Verlagsges München. 490 p. (In German).
- Assmann, E., 1955. Die Bedeutung des "erweiterten Eichhorn'schen Gesetzes" für die Konstruktion von Ertragstafeln [The importance of "extended Eichhorn's law" for the construction of yield tables]. *Forstw. Centralblatt* 74, 321–330 in German.
- Boisvenue, C., Running, S.W., 2006. Impacts of climate change on natural forest productivity – evidence since the middle of the 20th century. *Glob. Change Biol.* 12, 862–882. <https://doi.org/10.1111/j.1365-2486.2006.01134.x>.
- Bontemps, J.-D., Bouriaud, O., 2014. Predictive approaches to forest site productivity: recent trends, challenges and future perspectives. *Forest.: Int. J. Forest Res.* 87 (1), 109–128. <https://doi.org/10.1093/forestry/cpt034>.
- Brandel, G., 1990. Volume functions for individual trees; Scots pine (*Pinus sylvestris*), Norway spruce (*Picea abies*) and birch (*Betula pendula* and *Betula pubescens*). In: Department of Forest Yield Research, Swedish University of Agricultural Sciences, Garpenberg, pp. 183.
- Bueis, T., Bravo, F., Pando, V., Kissi, Y.-A., Turrión, M.-B., 2019. Phosphorus availability in relation to soil properties and forest productivity in *Pinus sylvestris* L. plantations. *Annals of Forest Science* 76, 97. <https://doi.org/10.1007/s13595-019-0882-3>.
- Burkhardt, H.E., Tomé, M., 2012. *Modelling forest trees and stands*. Springer Science and Business Media. Dordrecht.
- Cieszewski, C., Bailey, R.L., 2000. Generalized algebraic difference approach: Theory based derivation of dynamic site equations with polymorphism and variable asymptotes. *For. Sci.* 46, 116–126.
- Eckhart, T., Pötzelsberger, E., Koeck, R., Thom, D., Lair, G.J., van Loo, M., Hasenauer, H., 2019. Forest stand productivity derived from site conditions: an assessment of old Douglas fir stands (*Pseudotsuga menziesii* (Mirb.) Franco var. *menziesii*) in Central Europe. *Ann. For. Sci.* 76, 19. <https://doi.org/10.1007/s13595-019-0805-3>.
- Eichhorn, F., 1902. *Ertragstafeln für die Weißtanne* [Yield tables for the silver fir]. Verlag von Julius Springer, Berlin (in German).
- Ekö, P.-M., Johansson, U., Petersson, N., Bergqvist, J., Elfving, B., Frisk, J., 2008. Current growth differences of Norway spruce (*Picea abies*), Scots pine (*Pinus sylvestris*) and birch (*Betula pendula* and *Betula pubescens*) in different regions in Sweden. *Scand. J. Forest Res.* 23 (4), 307–318. <https://doi.org/10.1080/02827580802249126>.
- Ekö, P., 1985. A growth simulator for Swedish forests, based on data from the national forest survey. Department of Silviculture, Report 16, Swedish University of Agricultural Sciences. (in Swedish with English summary).
- Elfving, B., 2010a. Natural mortality in thinning and fertilisation experiments with pine and spruce in Sweden. *Forest Ecology and Management* 260, 353–360. [10.1016/j.foreco.2010.04.025](https://doi.org/10.1016/j.foreco.2010.04.025).
- Elfving, B., 2010b. Growth modelling in the Heureka system. Swedish University of Agricultural Sciences, Faculty of Forestry. [Online] (2011-03-29) Available from [http://heureka.slu.se/wiki/Heureka\\_prognosssystem\\_\(Elfving\\_rapportutkast\).pdf](http://heureka.slu.se/wiki/Heureka_prognosssystem_(Elfving_rapportutkast).pdf) [2021-03-10].
- Elfving, B., 2009. Height development functions. SLU, PM for Heureka, appendix 9, 2 pp.
- Elfving, B., Kiviste, A., 1997. Construction of site index equations for *Pinus sylvestris* L. using permanent plot data in Sweden. *For. Ecol. Manage.* 98 (2), 125–134.
- Elfving, B., Nyström, K., 1996. Yield capacity of planted *Picea abies* in northern Sweden. *Scand. J. Forest Res.* 11 (1-4), 38–49. <https://doi.org/10.1080/02827589609382910>.
- Elfving, B., Tegnhamar, L., 1996. Trends of tree growth in Swedish forests 1953–1992: An analysis based on sample trees from the National Forest Inventory. *Scand. J. Forest Res.* 11 (1-4), 26–37. <https://doi.org/10.1080/02827589609382909>.
- Fahlvik, N., Elfving, B., Wikström, P., 2014. Evaluation of growth functions used in the Swedish Forest Planning System Heureka. *Silva Fenn.* 48. [10.14214/sf.1013](https://doi.org/10.14214/sf.1013).
- Felton, A., Petersson, L., Nilsson, O., Witzell, J., Cleary, M., Felton, A.M., Björkman, C., Sang, Å.O., Jonell, M., Holmström, E., Nilsson, U., Rönnerberg, J., Kalén, C., Lindblad, M., 2019. The tree species matters: Biodiversity and ecosystem service implications of replacing Scots pine production stands with Norway spruce. *Ambio* 49 (5), 1035–1049. <https://doi.org/10.1007/s13280-019-01259-x>.
- Felton, A., Ranius, T., Roberge, J.-M., Öhman, K., Lämås, T., Hynynen, J., Juutinen, A., Mönkkönen, M., Nilsson, U., Lundmark, T., Nordin, A., 2017. Projecting biodiversity and wood production in future forest landscapes: 15 key modeling considerations. *J. Environ. Manage.* 197, 404–414. <https://doi.org/10.1016/j.jenvman.2017.04.001>.
- Fontes, L., Bontemps, J.-D., Bugmann, H., Van Oijen, M., Gracia, C., Kramer, K., Lindner, M., Rötter, T., Skovsgaard, J.P., 2010. Models for supporting forest management in a changing environment. *For. Syst.* 3 (4), 8. <https://doi.org/10.5424/fs/2010195-9315>.
- Fridman, J., Holm, S., Nilsson, M., Nilsson, P., Ringvall, A.H., Stahl, G., 2014. Adapting National Forest Inventories to changing requirements - the case of the Swedish National Forest Inventory at the turn of the 20th century. *Silva Fenn.* 48, 1095. [10.14214/sf.1095](https://doi.org/10.14214/sf.1095).
- Gadow, K.V., Hui, G., 1999. *Modelling Forest Development*, Forest Sciences. Springer Netherlands, Dordrecht. [10.1093/forestry/72.3.17](https://doi.org/10.1093/forestry/72.3.17).
- Gauthier, S., Bernier, P., Kuuluvainen, T., Shvidenko, A.Z., Schepaschenko, D.G., 2015. *Boreal forest health and global change*. *Science* 349 (6250), 819–822.
- Gregoire, T.G., Schabenberger, O., 1996. A non-linear mixed-effects model to predict cumulative bole volume of standing trees. *J. Appl. Stat.* 23 (2-3), 257–272. <https://doi.org/10.1080/02664769624233>.
- Hall, K.B., Stape, J., Bullock, B.P., Frederick, D., Wright, J., Scolforo, H.F., Cook, R., 2019. A Growth and Yield Model for *Eucalyptus benthamii* in the Southeastern United States. *For. Sci.* 66, 25–37. <https://doi.org/10.1093/forsci/fxz061>.
- Hasenauer, H., Burkhardt, H.E., Sterba, H., 1994. Variation in Potential Volume Yield of Loblobly Pine Plantations. *For. Sci.* 40, 162–176. <https://doi.org/10.1093/forestsce/40.1.162>.
- Hägglund, B., 1972. Site index curves for Norway spruce in northern Sweden. Swedish University of Agricultural Sciences, Department of Forest Yield Research, Report 21, pp. 1–298. (in Swedish with English summary).
- Hägglund, B., 1973. Site index curves for Norway spruce in southern Sweden. Swedish University of Agricultural Sciences, Department of Forest Yield Research, Report 24, pp. 1–49. (in Swedish with English summary).
- Hägglund, B., 1974. Site index curves for Scots pine in Sweden. Swedish University of Agricultural Sciences, Department of Forest Yield Research, Report 31, pp. 1–54. (in Swedish with English summary).
- Hägglund, B., Lundmark, J.E., 1977. Site index estimation by means of site properties. Scots pine and Norway spruce in Sweden. *Studia Forestalia Suecica*. pp. 38.

- Hägglund, B., 1981. Evaluation of forest site productivity. *For. Abst.* 42, 516–527.
- Hägglund, B., Lundmark, J.E., 1982. Handledning i bonitering med Skogshögskolans boniteringssystem. Swedish Forest Agency, Jönköping, Sweden, pp. 124. ISBN 91-857448-14-5. (in Swedish).
- Haworth, J., Vincent, P., 1982. Power-Transformations and Linear-Regression Models in Geography. *Area* 14, 137–143.
- Henttonen, H.M., Nöjd, P., Mäkinen, H., 2017. Environment-induced growth changes in the Finnish forests during 1971–2010—An analysis based on National Forest Inventory. *For. Ecol. Manage.* 386, 22–36. <https://doi.org/10.1016/j.foreco.2016.11.044>.
- Kauppi, P.E., Posch, M., Pirinen, P., 2014. Large Impacts of Climatic Warming on Growth of Boreal Forests since 1960. *PLoS One* 9. <https://doi.org/10.1371/journal.pone.0111340>.
- Levakovic, A., 1935. Analytical form of growth laws. *Glasnik za Sumske Pokuse (Zagreb)* 4, 189–282.
- Lizniewicz, M., Nilsson, U., Agestam, E., Eko, P.M., Elfving, B., 2016. A site index model for lodgepole pine (*Pinus contorta* Dougl. var. *latifolia*) in northern Sweden. *Scand. J. Forest Res.* 31, 583–591. <https://doi.org/10.1080/02827581.2016.1167238>.
- Liu, X., Duan, G., Chhin, S., Lei, X., Wang, D., Zhang, X., 2021. Evaluation of potential versus realized site productivity of *Larix principis-rupprechtii* plantations across northern China. *For. Ecol. Manage.* 479, 118608. <https://doi.org/10.1016/j.foreco.2020.118608>.
- Mäkinen, H., Henttonen, H.M., Kohnle, U., Kuehne, C., Nöjd, P., Yue, C., Klädtke, J., Siipilehto, J., 2021. Site carrying capacity of Norway spruce and Scots pine stands has increased in Germany and northern Europe. *For. Ecol. Manage.* 492, 119214. <https://doi.org/10.1016/j.foreco.2021.119214>.
- Mason, E.G., Holmstrom, E., Nilsson, U., 2017. Using hybrid physiological/mensurational modelling to predict site index of *Pinus sylvestris* L. in Sweden: a pilot study. *Scand. J. Forest Res.* 33, 147–154. <https://doi.org/10.1080/02827581.2017.1348539>.
- McRoberts, R.E., Westfall, J.A., 2016. Propagating uncertainty through individual tree volume model predictions to large-area volume estimates. *Ann. For. Sci.* 73 (3), 625–633. <https://doi.org/10.1007/s13595-015-0473-x>.
- Mehtätalo, L., Lappi, J., 2020. Biometry for Forestry and Environmental Data: With Examples in R. CRC Press.
- Näslund, M., 1947. Funktioner och tabeller för kubering av stående träd: Tall, gran och björk i södra Sverige samt i hela landet [Empirical formulae and tables for determining the volume of standing trees: Scots pine, Norway spruce and Birch in southern Sweden and in the whole country]. *Medd. Statens Skogsforskningsinst.* 36 (3), pp. 81. (in Swedish with English summary).
- Nilsson, P., 2020. Skogsdata (Official Forest Statistics of Sweden): aktuella uppgifter om de svenska skogarna från Riksskogstaxeringen. Tema: Den döda veden. Institutionen för skoglig resurshushållning, Umeå. Swedish University of Agricultural Sciences. (in Swedish with English summary).
- Nilsson, U., Elfving, B., Karlsson, K., 2012. Productivity of Norway spruce Compared to Scots Pine in the Interior of Northern Sweden. *Silva Fenn.* 46, 197–209. <https://doi.org/10.14214/sf.54>.
- Nilsson, U., Agestam, E., Ekö, P.-M., Elfving, B., Fahlvik, N., Johansson, U., Karlsson, K., Lundmark, T., Wallentin, C., 2010. Thinning of Scots pine and Norway spruce monocultures in Sweden (Report No. 219). Umeå.
- Nord-Larsen, T., Meilby, H., Skovsgaard, J.P., 2009. Site-specific height growth models for six common tree species in Denmark. *Scand. J. Forest Res.* 24 (3), 194–204. <https://doi.org/10.1080/02827580902795036>.
- Peschel, W., 1938. Die mathematischen Methoden zur Herleitung der Wachstumsgesetze von Baum und Bestand und die Ergebnisse ihrer Anwendung [The mathematical methods for deriving the growth laws of trees and stands and the results of their application]. *Tharandter Forstl. Jahrb.* 89, 169–247 [In German].
- Pettersson, N., 1992. The effect of spacing on volume and structure in planted Scots pine and Norway spruce stands. SLU, Dept. of Forest Growth and Yield. Report 30 (58 pp).
- Pienaar, L.V., Page, H., Rheney, J.W., 1990. Yield prediction for mechanically site-prepared slash pine plantations. *Southern J. Appl. Forest.* 14 (3), 104–109.
- Pienaar, L.V., Shiver, B.D., 1986. Basal Area Prediction and Projection Equations for Pine Plantations. *For. Sci.* 32, 626–633. <https://doi.org/10.1093/forests/32.3.626>.
- Pinheiro, J., Bates, D., DebRoy, S., Sarkar, D., Core Team, R., 2020. Nlme: Linear and Nonlinear Mixed Effects Models. R package version 3, 1–148. <https://CRAN.R-project.org/package=nlme>.
- Pretzsch, H., del Río, M., Biber, P., Arcangeli, C., Bielak, K., Brang, P., Dudzinska, M., Forrester, D.I., Klädtke, J., Kohnle, U., Ledermann, T., Matthews, R., Nagel, J., Nagel, R., Nilsson, U., Ningre, F., Nord-Larsen, T., Wernsdorfer, H., Sycheva, E., 2019. Maintenance of long-term experiments for unique insights into forest growth dynamics and trends: review and perspectives. *Eur. J. For. Res.* 138 (1), 165–185. <https://doi.org/10.1007/s10342-018-1151-y>.
- Pretzsch, H., Grote, R., Reineking, B., Rötzer, T.H., Seifert, S.T., 2008. Models for Forest Ecosystem Management: A European Perspective. *Ann. Bot.* 101, 1065–1087. <https://doi.org/10.1093/aob/mcm246>.
- R Core Team, 2020. R: A language and environment for statistical computing. R Foundation for Statistical Computing, Vienna, Austria. Retrieved from <https://www.R-project.org/>.
- Richards, F.J., 1959. A Flexible Growth Function for Empirical Use. *J. Exp. Bot.* 10 (2), 290–301. <https://doi.org/10.1093/jxb/10.2.290>.
- Samuelson, L.J., Eberhardt, T.L., Butnor, J.R., Stokes, T.A., Johnsen, K.H., 2010. Maximum growth potential in loblolly pine: results from a 47-year-old spacing study in Hawaii. *Can. J. For. Res.* 40 (10), 1914–1929. <https://doi.org/10.1139/X10-133>.
- Schmidt, A., 1973. Ertragsniveau und Standort dargestellt am Beispiel der Kiefer [Yield level and allocation shown using the example of pine]. *Forstwiss. Centrallbl.* 92 (1), 268–274.
- Schumacher, F.X., 1939. A new growth curve and its application to timber-yield studies. *J. Forest.* 37, 819–820.
- Sharma, R.P., Brunner, A., Eid, T., 2012. Site index prediction from site and climate variables for Norway spruce and Scots pine in Norway. *Scand. J. Forest Res.* 27 (7), 619–636. <https://doi.org/10.1080/02827581.2012.685749>.
- Skovsgaard, J.P., Vanclay, J.K., 2008. Forest site productivity: a review of the evolution of dendrometric concepts for even-aged stands. *Forestry* 81, 13–31. <https://doi.org/10.1093/forestry/cpm041>.
- Skovsgaard, J.P., 1997. Management of Sitka Spruce without Thinnings. An Analysis of Stand Structure and Volume Production of Unthinned Stands of Sitka Spruce (*Picea sitchensis* (Bong.) Carr.) in Denmark. *Forskningscentret for Skov & Landskab, Forskningsserien*, Hørsholm, Vol. 19.
- Sterba, H., Monserud, R.A., 1995. Potential Volume Yield for Mixed-Species Douglas-Fir Stands in the Northern Rocky Mountains. *For. Sci.* 41, 531–545. <https://doi.org/10.1093/forests/41.3.531>.
- Sterba, H., 1987. Estimating Potential Density from Thinning Experiments and Inventory Data. *For. Sci.* 33, 1022–1034. <https://doi.org/10.1093/forests/33.4.1022>.
- Szwaluk, K.S., Strong, W.L., 2003. Near-surface soil characteristics and understory plants as predictors of *Pinus contorta* site index in southwestern Alberta, Canada. *For. Ecol. Manage.* 176 (1–3), 13–24. [https://doi.org/10.1016/S0378-1127\(02\)00228-1](https://doi.org/10.1016/S0378-1127(02)00228-1).
- Ung, C.-H., Ouellet, D., 1991. Stand volume tables: Application to black spruce stands of Lebel-sur-Quévillon. *Forest. Chron.* 67 (6), 712–715. <https://doi.org/10.5558/tfc67712-6>.
- von Bertalanffy, L., 1938. A quantitative theory of organic growth (Inquiries on growth laws. II). *Hum. Biol.* 10, 181–213.
- Wikström, P., Edenius, L., Elfving, B., Eriksson, L.O., Lämås, T., Sonesson, J., Öhman, K., Wallerman, J., Waller, C., Klintebäck, F., 2011. The Heureka forestry decision support system: an overview. *Math. Comput. Forest. Natural-Resour. Sci.* 3 (2), 87–94.